Local Non-similarity Solution for some Two-dimensional Boundary Layer Flows

Submitted by

ARSLAN QADEER

779-FBAS/MSMA/F21

Department of Mathematics and Statistics

Faculty of Sciences

International Islamic University, Islamabad Pakistan

2023

TM-27042 km

NIS
532.051
PK

Boundary layers
Differential equations, Partial
Fluid dynamics - Mathematical models
Similarity solutions
Mathematical analysis

Local Non-similarity Solution for some Two-dimensional Boundary Layer Flows

Submitted by

ARSLAN QADEER

779-FBAS/MSMA/F21

Supervised by

Prof. Dr. Nasir Ali

Department of Mathematics and Statistics

Faculty of Sciences

International Islamic University, Islamabad Pakistan

2023

Local Non-similarity Solution for some Two-dimensional Boundary Layer Flows

Submitted by

ARSLAN QADEER

779-FBAS/MSMA/F21

A Thesis

Submitted in the Partial Fulfillment of the

Requirements for Degree of

MASTER OF SCIENCE

IN

MATHEMATICS

Supervised by

Prof. Dr. Nasir Ali

Department of Mathematics and Statistics

Faculty of Sciences

International Islamic University, Islamabad Pakistan

2023

Certificate

Local Non-similarity Solution for some Two-dimensional Boundary Layer Flows

By:

Arslan Qadeer

A dissertation submitted in the partial fulfillment of the requirements for the degree of the **Master of Science in Mathematics**

We accept this dissertation as conforming to the required standard.

1. _____
Dr. Qazi Muhammad Zaigham Zia,
External Examiner

2. _____
Dr. Ahmed Zeeshan
Internal Examiner

3. _____
Prof. Dr. Nasir Ali
Supervisor

4. _____
Prof. Dr. Nasir Ali
Chairman

Department of Mathematics & Statistics
Faculty of Sciences
International Islamic University, Islamabad
Pakistan
2023

A thesis submitted to Department of Mathematics,
Faculty of Sciences, International Islamic University,
Islamabad as a partial fulfillment of requirement for
the award of the Degree of MS Mathematics.

DECLARATION

I hereby declare that the work presented in this thesis is my own effort, except where otherwise acknowledged and that the thesis is my own composition. No part of the thesis has been previously presented for any other degree.

Date 14-09-23

Arslan

Arslan Qadeer

MS in Mathematics

779-FBAS/MSMA/F21

DEDICATION

I dedicate this Thesis to

Hazrat Muhammad (S.A.W),

My Teachers

And

My Parents.

Acknowledgements

In the name of Allah, the most gracious and the most merciful. First and foremost, I am thankful to Almighty **ALLAH** for guided us on the path of knowledge after creating us as human being. And giving me the strength, knowledge, ability and opportunity to undertake this study and complete it satisfactorily.

Secondly, I would like to thank my respected teacher and supervisor, **Prof. Dr. Nasir Ali** who's worthy guidance and professional attitudes appreciable in completing this dissertation.

I am extremely grateful to my advisor **Mr. Qamar Zaman** for his support throughout this process. He was the man who guided us completely from the beginning to the end of the research, his encouragement, observation, attitude and support of kindness meant a lot. I thank to my fellows and friends who deserve formal acknowledgement but could not be named individually.

I am extremely grateful to **My Parents** and **Siblings** for their support, encouragement and genuine interest in my academic success. The selfless prayers and good wishes of my parents have always been the source of my success in all aspects of my life. I am also thankful to **My Father** for his moral support.

Arslan Qadeer

779-FBAS/MSMA/F21

PREFACE

Fluid mechanics is a prominent area of interest in engineering and applied sciences. Its wide-ranging applications in energy systems, aerospace, and materials processing have attracted the attention of many researchers.

Specifically, the investigation of boundary layer fluids has gained significant importance, as scholars seek novel approaches to analyze their behavior under diverse flow conditions. This MS thesis focuses on the examination of the local non-similarity solution method for some boundary layer flows.

The first chapter of this thesis provides an introduction to the local non-similarity solution method, covering the fundamental concepts and relevant definitions. It lays the foundation for the subsequent chapters, offering a comprehensive understanding of the theoretical framework underlying stability analysis in fluid flows.

The second chapter presents a meticulous review of the existing literature on the local non-similarity solution method. This chapter aims to provide a comprehensive summary of the key findings and methodologies employed in the analysis of these flows, providing valuable context for the subsequent chapters.

The third chapter represents the core of this thesis, where I present my own work on the local non-similarity solution method for the flow of a Williamson fluid over a Stretching Sheet. Building upon the knowledge and methodologies established in the preceding chapters, I analyze the local non-similarity solution method and compare the results with the numerical solution method. By employing theoretical models, numerical simulations, and rigorous mathematical techniques, I aim to shed light on the stability behavior of this flow and contribute to the existing body of knowledge in the field.

This research endeavor is the culmination of countless hours of analysis, computation, and reflection. I sincerely hope that this thesis will serve as a valuable resource for researchers, engineers, and students alike who are interested in the field of fluid dynamics and stability analysis. I believe that a deeper understanding of the stability properties of fluid flows will contribute to the

development of more efficient and reliable engineering designs and enhance our understanding of the complex dynamics of fluid systems.

Finally, I would like to express my appreciation to my family and friends for their unwavering belief in my abilities and their constant encouragement. Their love and support have been a constant source of motivation, without which this thesis would not have been possible.

I sincerely hope that the findings and insights presented in this thesis will pave the way for further advancements in the field of stability analysis of fluid flows, ultimately contributing to the broader scientific and engineering community.

Contents

List of Tables

List of plots

Nomenclature

α	Thermal diffusivity
χ	$\frac{\partial \phi}{\partial \xi}$
η	Pseudo-similarity variable
λ	Porosity parameter
ν	Kinematic viscosity
ϕ	$\frac{\partial \theta}{\partial \xi}$
ψ	Stream function
ρ	Density of fluid
θ	Dimensionless temperature variable
ξ	Transformed variables
f	Reduced stream function
g	$\frac{\partial f}{\partial \xi}$
h	$\frac{\partial g}{\partial \xi}$
Nu_x	Local Nusselt number
pr	Prandtl number
R	Radius of the cylinder
Re_x	Local Reynolds number
T	Temperature
T_∞	Free-stream temperature
T_w	Wall temperature
u,v	Velocity components
U_∞	Free stream velocity
v_w	Surface velocity

We	Local Weissenberg number
x	Stream-wise coordinate
y	Transverse coordinate

Chapter 1

Introduction

Fluid mechanics is a complex discipline that analyzes the behavior of fluids. In the real world, many fluid flows behave differently from one another, and these non-similar flows cannot be analyzed using traditional scaling principles based on similarity characteristics like Reynolds number. As a result, more sophisticated mathematical techniques are required to analyze non-similar flows. There are several techniques for solving non-similar flows, including numerical techniques, perturbation techniques, and asymptotic techniques. Each approach has its own advantages and disadvantages, and the best approach depends on the specific problem. In the case of two-dimensional flows, the local non-similarity technique is often preferred because it can provide analytical solutions for non-similar flows in a local area surrounding a particular point of interest. The goal of this thesis is to examine local non-similar solutions for a few two-dimensional flows and use the local non-similarity solution method to analyze their behavior. By studying local non-similar solutions for these flows, it may be possible to develop more reliable and efficient systems. We will also investigate the importance of choosing the right boundary conditions when trying to solve non-similar flows. Overall, this thesis will improve our understanding of non-similar flows and the local non-similarity approach for their analysis, which is essential for many real-world engineering applications.

1.0.1 Fluid

A substance that lacks a definite shape and readily responds to external pressure, whether it be a gas or, particularly, a liquid, is referred to as a fluid.

1.0.2 Types of fluid

Fluids can be classified into two main types:

Newtonian fluids

Newtonian flows are fluids whose viscosity is independent of the shear rate. Water and air are examples of Newtonian fluids.

Non-Newtonian fluids

Non-Newtonian fluids are fluids whose viscosity is not constant. The viscosity of a non-Newtonian fluid can change depending on the shear rate, which is the rate at which the fluid is deformed.

1.0.3 Fundamental laws (Conservation laws)

Conservation of Mass

The Conservation of Mass principle states that within a closed system, the total mass remains constant over time. Mathematically, this is expressed as the following equation:

$$\frac{\partial \rho}{\partial t} + \nabla \cdot (\rho \mathbf{v}) = 0,$$

Here, ρ represents the density of the fluid, $\mathbf{v}$ is the fluid velocity, t stands for time, and ∇ denotes the gradient operator. This equation embodies the fundamental concept of mass preservation and asserts that the rate of change of mass within a fluid element equals the divergence of the mass flow across its boundary.

Conservation of Momentum

Conservation of Momentum states that the total momentum of an isolated system remains constant over time unless influenced by external forces. This is expressed mathematically as:

$$\rho \left(\frac{\partial \mathbf{v}}{\partial t} + \mathbf{v} \cdot \nabla \mathbf{v} \right) = -\nabla p + \mu \nabla^2 \mathbf{v} + \mathbf{f},$$

Here, ρ represents fluid density, $\mathbf{v}$ is the fluid velocity, t is time, p is fluid pressure, μ is fluid viscosity, ∇ is the gradient operator, and $\mathbf{f}$ is the external force. This equation embodies the fundamental principle of momentum conservation, indicating that the rate of momentum change within a fluid element is equal to the combined effects of the pressure gradient, viscous forces, and external forces.

Conservation of Energy

The Conservation of Energy states that energy within a system remains constant over time, transforming between different forms but never being created or destroyed. This is expressed mathematically as:

$$\frac{\partial (\rho E)}{\partial t} + \nabla \cdot (\rho \mathbf{E} \mathbf{v}) = -\nabla \cdot \mathbf{q} + \nabla \cdot (\boldsymbol{\sigma} \mathbf{v}) + S,$$

Here, ρ is the density of the fluid, E is the total energy per unit mass, $\mathbf{v}$ is the fluid velocity, t is time, $\mathbf{q}$ is the heat flux, $\boldsymbol{\sigma}$ is the stress tensor, and S represents an external heat source or sink.

1.0.4 Boundary layer flow

Boundary layer flow refers to the motion of fluid adjacent to a solid surface, characterized by a thin region where the velocity changes significantly. It occurs when a fluid

flows over a surface, such as air flowing over an aircraft wing or water flowing over a ship's hull. The boundary layer is important in understanding the aerodynamic or hydrodynamic behavior of the flow, as it affects factors like drag, heat transfer, and the overall performance of the system. This phenomenon is widely studied in various fields, including aerospace engineering, fluid dynamics, and meteorology.

1.0.5 Boundary layer equations

The simplified equations for a steady flow in the boundary layer can be written as:

Conservation of Mass:

$$u_x + v_y = 0,$$

Conservation of Momentum:

$$u_t + uu_x + vu_y = \frac{1}{\rho}\frac{\partial p}{\partial x} + \nu(u_{xx} + u_{yy}),$$

$$u_t + uv_x + vv_y = \frac{1}{\rho}\frac{\partial p}{\partial x} + \nu(v_{xx} + v_{yy}),$$

Conservation of Energy:

$$T_t + uT_x + vT_y = \frac{\alpha}{\rho c_p}(T_{xx} + T_{yy}),$$

Here, u and v are the velocity components along the x and y axes, respectively. The variables T, p, ρ, ν, α, and c_p stand for pressure, temperature, fluid density, fluid thermal diffusivity, kinematic viscosity, and specific heat at constant pressure, respectively.

1.0.6 Thermal Boundary layer

The thermal boundary layer refers to the thin layer of fluid near a solid surface where heat transfer significantly affects the temperature distribution, particularly in fluid dynamics contexts.

1.0.7 Williamson fluid

Williamson fluid is a non-Newtonian fluid that exhibits both shear-thinning and viscoelastic properties. It is used to model fluids that have yield stress, such as slurries, gels, and emulsions. The mathematical equation for two-dimensional Williamson fluid [1] is:

$$\mathbf{S} = -p\mathbf{I} + \boldsymbol{\tau},$$

and,

$$\boldsymbol{\tau} = \left[\mu_\infty + \frac{(\mu_0 - \mu_\infty)}{1 + \Gamma|\dot{\gamma}|}\right]\mathbf{A}_1.$$

1.0.8 Self-similar flow

Self-similar flow refers to a type of flow in which the flow properties remain unchanged when the spatial coordinates are scaled by a constant factor. In other words, the flow pattern repeats itself at different scales. In self-similar flows, the external potential velocity follows a power law or exponential function.

1.0.9 Non-similar flow

Non-similar flow occurs when the external potential velocity is not a power law or exponential function. To solve non-similar flows, similarity transformations are still required, but the dimensionless stream function is assumed to be a function of both a similarity variable and the spatial coordinate. The coefficients of the derivative terms in the transformed momentum equations depend on both the similarity variable and the spatial coordinate.

Boundary conditions in non-similar flows

Boundary conditions are the set of equations that describe the behavior of the fluid at the boundary of the domain under consideration. The fulfillment of these conditions is essential for obtaining a unique solution to the non-similar flow problem. The boundary conditions for non-similar flows depend on the type of flow and the geometry of the problem.

Importance of choosing appropriate boundary conditions

The choice of appropriate boundary conditions is critical in non-similar flow solutions as incorrect boundary conditions can lead to physically unrealistic solutions. For example, in a flow with a stagnation point,The fluid velocity is zero at the stagnation point. If the boundary conditions are not appropriately set, the solution obtained may have non-zero velocity at the stagnation point, which is physically unrealistic. In addition, appropriate boundary conditions can also help in reducing the computational effort required to solve non-similar flow problems. By setting appropriate boundary conditions, the size of the computational domain can be reduced, which can significantly reduce the computational cost of the solution.

Boundary conditions for specific types of non-similar flows

Different types of non-similar flows require different boundary conditions for their solution. For example, in a boundary layer flow, the velocity of the fluid at the surface is zero, and the velocity profile is assumed to follow a specific law. In a free shear layer, the velocity of the fluid is not zero at the boundary, and the boundary conditions depend on the type of shear layer.

1.0.10 Methods for solving non-similar flows

The most commonly used methods for solving non-similar flows are:

Numerical methods

Discretizing the governing equations and solving them using a computer is known as numerical methods. These methods are useful for solving complex non-linear systems and are widely used in computational fluid dynamics (CFD). Finite difference, finite element, and finite volume methods are examples of numerical methods used for solving non-similar flows.

Perturbation methods

Perturbation methods involve breaking down the governing equations into a series of equations that can be solved iteratively. These methods are useful when the solution to the governing equations is not known but is close to a known solution. Perturbation methods are commonly used in the analysis of small perturbations of known solutions. Boundary layer theory and Stokes expansion are examples of perturbation methods used for solving non-similar flows.

Asymptotic methods

Asymptotic methods involve approximating the solution to the governing equations using a series of simpler equations. These methods are useful when the governing equations are complex, and an analytical solution is not possible. Asymptotic methods are widely used in the analysis of boundary layer flows. The method of matched asymptotic expansions and the method of multiple scales are examples of asymptotic methods used for solving non-similar flows.

Local non-similarity solution method

The local non-similarity solution method involves approximating the solution to the governing equations using simpler equations that are valid in a local region around a specific point of interest. This method is useful for analyzing flows that exhibit boundary layers or stagnation points, which are common features in many engineering applications. The local non-similarity solution method provides analytical solutions for non-similar flows in a local region and is widely used in the analysis of two-dimensional flows.

1.0.11 Local non-similarity solution method

The local non-similarity solution method describes fluid flows near a specific point on a surface that cannot be approximated by a self-similar flow. This may occur due to various factors, such as surface roughness, changes in the flow direction, or other complex flow phenomena. In these cases, it is necessary to use more complex mathematical models to describe the behavior of the fluid flow near the point of interest. local non-similarity solution method methods often involve additional variables and partial differential equations to account for the variations in flow properties near the point of interest.

1.0.12 Principles of the local non-similarity solution method

The local non-similarity solution method is a mathematical technique for solving fluid flow problems in boundary layers that do not follow a simple mathematical function. The method approximates the velocity profiles in the boundary layer by a power law and solves the governing equations for the flow, subject to appropriate boundary conditions.

1.0.13 Applications of the local non-similarity solution method

The local non-similarity solution method is a highly adaptable technique for examining fluid flows in diverse fields, encompassing aerodynamics, heat transfer, and chemical

engineering. Among its significant utilities lies its invaluable role in the scrutiny of boundary layers within two-dimensional flows. This method enables the determination of boundary layer thickness as well as velocity profiles, crucial factors in the design of various systems like aircraft wings and heat exchangers. Furthermore, the local non-similarity solution method can be effectively employed in the analysis of flows featuring stagnation points, a prevalent occurrence in numerous engineering applications.

1.0.14 Benefits of the local non-similarity solution method

The technique of employing the local non-similarity solution method offers numerous advantages compared to alternative approaches when examining non-similar flows. A key strength lies in its capacity to furnish analytical solutions, which frequently hold greater utility for engineering design purposes than numerical solutions. Additionally, the method proves relatively straightforward to implement and facilitates the computation of pivotal parameters like the Reynolds number and the Nusselt number. These parameters play a crucial role in the design of efficient systems.

1.0.15 Limitations of the local non-similarity solution method

The local non-similarity solution method has some limitations that should be considered when applying it to real-world problems. One of its limitations is that it is only applicable in a local region around a specific point of interest. This means that the method cannot provide a global solution for the flow field. Additionally, the method assumes that the flow is steady and laminar, which may not be the case in all real-world applications.

1.0.16 Literature Review

The study of the local non-similarity solution method has gained significant attention in the field of fluid mechanics and heat transfer. Local non-similar solutions involve solving boundary-layer problems where similarity solutions are not applicable due to varying physical parameters. This literature review critically analyzes and summarizes relevant academic literature on the topic, identifies gaps or inconsistencies, and highlights the significance of studying local non-similarity solution method. The Local Nonsimilarity Solutions (LNS) method, introduced by Sparrow et al. [2], to find the locally non-similar velocity boundary layer. Later, sparrow and YU [3] implemented this method for obtaining local non-similar solution for the thermal boundary layer. Later this method was employed by various researchers to obtain locally non-similar solutions for a variety of velocity and thermal boundary layers. A brief review of such an investigation is presented below. Minkowycz and Sparrow [4] used the LNS method to solve natural convection on a vertical cylinder, especially when the results were significantly different from those on a flat surface. They ensured accuracy by examining the governing equations at different levels of detail. Hossain et al. [5] looked at fluid flow over a wedge, considering factors like convective inertia, solid boundaries, porous inertia, and Darcy flow resistance. They used three different methods, including the LNS method, to solve the complex equations for momentum and thermal boundary layers, and compared the results extensively. Massoudi [6] studied the flow of a power-law fluid over a wedge, finding both similar and non-similar solutions for velocity and

temperature fields. Yian and Amin [7] incorporate the consideration of nonsimilarity terms present within the momentum and energy equations. These terms, which have previously been overlooked in methods like similarity and local similarity approaches, are now taken into account. Mohamad [8] explored the impact of different types of nanoparticles on boundary layer flow and heat transfer in an incompressible nanofluid along a permeable vertical plate with thermal radiation in the presence of a magnetic field, obtaining non-similar solutions for velocity and temperature fields. Khamis [9] investigated the convective heat transfer in a steady flow of an electrically conducting fluid over a porous wedge with uniform suction or injection. This led to a locally nonsimilar flow field, described by nonsimilar ordinary differential equations. Afridi et al. [10] used the LNS method to study non-similar MHD mixed convection flow in the presence of energy dissipation and Joule heating, deriving equations and obtaining non-similar solutions for velocity and temperature fields. Sardar et al. [11] studied non-similar solutions for the two-dimensional steady Carreau fluid flow in the presence of a magnetic field and mixed convection of infinite shear rate viscosity using the local non-similarity solution method, resulting in non-similar solutions for velocity and temperature fields. Our objective is to apply the local non-similarity method to study the flow behavior of Williamson fluid over a stretched sheet. Despite its inherent non-similar characteristics, many researchers mistakenly treat Williamson fluid as exhibiting similar behavior [12, 13, 14, 15]. In contrast, we acknowledge and treat it as a non-similar flow and employ the local non-similarity method to solve the governing equations. Subsequently, we aim to compare the results obtained from the local non-similarity method with those derived from numerical methods to validate the accuracy and efficacy of our approach.

Chapter 2

Local Non-Similarity Thermal Boundary-Layer Solutions

Introduction

The local non-similarity solution method has been applied to the thermal boundary layer flow in this chapter. This flow exhibits non-similarity due to four factors surface mass transfer, transverse curvature, streamwise variation of free stream velocity, and streamwise variation of surface temperature. The local non-similarity solution method effectively transforms the governing partial differential equations into ordinary differential equations. Three truncations were implemented to simplify the ODEs, and the bvp4c numerical method was utilized to solve them. The results of the numerical simulations demonstrate the accurate predictive capability of the local non-similarity solution method for the behavior of thermal boundary layer flow. The impacts of the four non-similarity factors were comprehensively analyzed and discussed.

2.0.1 Surface Mass Transfer

Mathematical formulation

Let us consider a flat plate that is parallel to a uniform stream of fluid. The x-axis is the streamwise coordinate and the y-axis is the transverse coordinate. If the wall velocity, v_w , is proportional to x^ω , then the problem admits a similarity solution. Otherwise, the problem does not admit a similarity solution.

Thermal non-similarity in this case arises due to the velocity. The non-uniform velocity profile in the boundary layer results in a non-uniform temperature profile. The governing equations are as follows:

$$u_x + v_y = 0, \tag{2.1}$$

$$uu_x + vu_y = \nu u_{yy}, \tag{2.2}$$

$$uT_x + vT_y = \alpha T_{yy}. \tag{2.3}$$

In this particular scenario, the velocity component aligned with the flow direction is denoted as u, whereas the velocity component perpendicular to the flow is denoted as v. The temperature is represented by T, and the kinematic viscosity and thermal

diffusivity are indicated by α and ν, respectively. The prescribed conditions at the boundaries are provided as follows:

$$\begin{aligned} at\ y = 0 :\ u = 0,\ v = v_w\ ,\ T = T_w \\ at\ y \to \infty :\ u = U_\infty\ ,\ T = T_\infty. \end{aligned} \tag{2.4}$$

In order to derive the solution for the governing equations, it is necessary to transform the x,y coordinate system into the ξ and η coordinate system. This is because the governing equation can be more easily solved in the ξ and η coordinate systems.

The transformation from x,y to ξ and η can be done using the following similarities:

$$\eta = y\sqrt{\frac{U_\infty}{2\nu x}}, \quad \xi = (\frac{v_w}{U_\infty})\sqrt{\frac{2U_\infty}{\nu}}.$$

In simpler terms, the chosen value of η is associated with the reduced stream function ψ, while θ represents a temperature that has been scaled to remove any dimensional units, that is

$$f(\xi,\eta) = \frac{\psi}{\sqrt{2\nu x U_\infty}}, \quad \theta(\xi,\eta) = \frac{T - T_\infty}{T_w - T_\infty}.$$

The system of equations (2.1)-(2.4) can be solved by introducing a new function called the stream function $\psi(\xi,\eta)$, which relates to the velocity components as follows:

$$u = \frac{\partial\psi}{\partial y} \quad and \quad v = \frac{-\partial\psi}{\partial x}, \tag{2.5}$$

To find the values of u and v, which are respectively defined as $u = \frac{\partial\psi}{\partial y}$ and $v = \frac{-\partial\psi}{\partial x}$, the initial step is to calculate $\frac{\partial\psi}{\partial y}$ and $\frac{-\partial\psi}{\partial x}$. As

$$\psi = f(\xi,\eta)\sqrt{2\nu x U_\infty}. \tag{2.6}$$

The derivative of equation (2.6) with respect to y is:

$$\frac{\partial\psi}{\partial y} = \frac{\partial}{\partial y}(f(\xi,\eta)\sqrt{2\nu x U_\infty}),$$

$$= \sqrt{2\nu x U_\infty}(\frac{\partial f}{\partial\xi}\frac{\partial\xi}{\partial y} + \frac{\partial f}{\partial\eta}\frac{\partial\eta}{\partial y}),$$

After solving, the solution is

$$\frac{\partial\psi}{\partial y} = U_\infty\frac{\partial f}{\partial\eta},$$

or

$$u = U_\infty\frac{\partial f}{\partial\eta}, \tag{2.7}$$

and, differentiating equation (2.6) with respect to x gives

$$\frac{\partial\psi}{\partial x} = \frac{\partial}{\partial x}(f(\xi,\eta)\sqrt{2\nu x U_\infty}),$$

$$= \sqrt{2\nu x U_\infty}(\frac{\partial f}{\partial\xi}\frac{\partial\xi}{\partial x} + \frac{\partial f}{\partial\eta}\frac{\partial\eta}{\partial x}),$$

$$= v_w \frac{\partial f}{\partial \xi} + \sqrt{\frac{\nu U_\infty}{2x}}(f(\xi,\eta) - \eta \frac{\partial f}{\partial \xi}).$$

As

$$v = \frac{-\partial \psi}{\partial x},$$

$$v = \sqrt{\frac{\nu U_\infty}{2x}}(\eta \frac{\partial f}{\partial \xi} - f(\xi,\eta)) - v_w \frac{\partial f}{\partial \xi}. \tag{2.8}$$

In the context of this system, equation (2.1) for the conservation of mass is always satisfied without exception. Substituting (2.7) and (2.8) into (2.2) results in

$$U_\infty v_w \sqrt{\frac{U_\infty}{2x\nu}}(\frac{\partial f}{\partial \eta}\frac{\partial^2 f}{\partial \eta \partial \xi} - \frac{\partial^2 f}{\partial \eta^2}\frac{\partial f}{\partial \xi}) - \frac{U_\infty^2}{2x}\frac{\partial^2 f}{\partial \eta^2} f = \frac{U_\infty^2}{2x}\frac{\partial^3 f}{\partial \eta^3}. \tag{2.9}$$

Multiplication of $\frac{2x}{U_\infty^2}$ to both sides of equation (2.9) gives

$$\frac{v_w}{U_\infty}\sqrt{\frac{2xU_\infty}{\nu}}(\frac{\partial f}{\partial \eta}\frac{\partial^2 f}{\partial \eta \partial \xi} - \frac{\partial^2 f}{\partial \eta^2}\frac{\partial f}{\partial \xi}) - f\frac{\partial^2 f}{\partial \eta^2} = \frac{\partial^3 f}{\partial \eta^3},$$

or

$$\frac{\partial^3 f}{\partial \eta^3} + f\frac{\partial^2 f}{\partial \eta^2} = \xi(\frac{\partial f}{\partial \eta}\frac{\partial^2 f}{\partial \eta \partial \xi} - \frac{\partial^2 f}{\partial \eta^2}\frac{\partial f}{\partial \xi}), \tag{2.10}$$

with

$$f + \xi = -\xi \frac{\partial f}{\partial \xi}, \quad f'(\xi,0) = 0, \quad f'(\xi,\infty) = 1. \tag{2.11}$$

As

$$\theta(\xi,\eta) = \frac{T - T_\infty}{T_w - T_\infty},$$

$$T = \theta(\xi,\eta)(T_w - T_\infty) + T_\infty,$$

Differentiating with respect to x and y

$$\frac{\partial T}{\partial x} = Ax^\lambda \frac{v_w}{U_\infty}\sqrt{\frac{U_\infty}{2\nu x}}\frac{\partial \theta}{\partial \xi} - \frac{Ax^\lambda}{2x}\eta\theta' + \theta A\lambda x^{\lambda-1}, \tag{2.12}$$

$$\frac{\partial T}{\partial y} = Ax^\lambda \sqrt{\frac{U_\infty}{2\nu x}}\theta', \tag{2.13}$$

By substituting (2.7), (2.8), (2.12), and (2.13) into (2.3), the resulting expression is

$$Ax^\lambda v_w \sqrt{\frac{U_\infty}{2\nu x}}(\frac{\partial f}{\partial \eta}\frac{\partial \theta}{\partial \xi} - \frac{\partial \theta}{\partial \eta}\frac{\partial f}{\partial \xi}) + \frac{U_\infty \lambda A x^\lambda}{x}\frac{\partial f}{\partial \eta}\theta - \frac{U_\infty A x^\lambda}{2x} f\theta' = \frac{U_\infty A x^\lambda}{2Prx}\frac{\partial^2 \theta}{\partial \eta^2}, \tag{2.14}$$

where, $Pr = \frac{\nu}{\alpha}$

$$(\frac{1}{Pr})\frac{\partial^2 \theta}{\partial \eta^2} + f\frac{\partial \theta}{\partial \eta} - 2\lambda \frac{\partial f}{\partial \eta}\theta = \xi(\frac{\partial f}{\partial \eta}\frac{\partial \theta}{\partial \xi} - \frac{\partial \theta}{\partial \eta}\frac{\partial f}{\partial \xi}), \tag{2.15}$$

with

$$\theta(\xi,0) = 1, \quad \theta(\xi,\infty) = 0. \tag{2.16}$$

Equations (2.10) and (2.15) can be restated as:

$$f''' + ff'' = \xi(f'\frac{\partial f'}{\partial \xi} - f''\frac{\partial f}{\partial \xi}), \tag{2.17}$$

$$(\frac{1}{Pr})\theta'' + f\theta' - 2\lambda\, f'\theta = \xi(f'\frac{\partial \theta}{\partial \xi} - \theta'\frac{\partial f}{\partial \xi}), \tag{2.18}$$

with

$$f + \xi = -\xi\frac{\partial f}{\partial \xi}, \quad f'(\xi,0) = \theta(\xi,\infty) = 0, \quad f'(\xi,\infty) = \theta(\xi,0) = 1. \tag{2.19}$$

1st Level of Truncation (Local Similarity)

Before using the method of local non-similarity, it is helpful to first understand the method of local similarity . This method assumes that the terms on the RHS of equations (2.17), (2.18), and (2.19) are negligible, which allows the boundary-layer equations and boundary conditions to be simplified as

$$f''' + ff'' = 0, \tag{2.20}$$

$$(\frac{1}{Pr})\theta'' + f\theta' - 2\lambda\, f'\theta = 0, \tag{2.21}$$

with

$$f = -\xi, \quad f'(\xi,0) = \theta(\xi,\infty) = 0, \quad f'(\xi,\infty) = \theta(\xi,0) = 1. \tag{2.22}$$

Here, ξ is the constant parameter in the streamwise direction. Equations (2.20) and (2.21) can be approached as ordinary differential equations and solved using established methods suitable for similarity boundary layers. It is important to note that the solution for a specific value of ξ remains unaffected by the solution at any other value of ξ. However, with increasing values of ξ, the accuracy of the outcomes becomes uncertain, and for high injection rates (large ξ), the precision significantly diminishes.

2nd Level of Truncation (Local Non-Similarity)

This level involves retaining the governing equations for f and θ (Eqs. 2.17 and 2.18) without making any approximations. The variables $\frac{\partial f}{\partial \xi} = g$ and $\frac{\partial \theta}{\partial \xi} = \phi$ are then introduced. When g and ϕ are applied, equation (2.17)-(2.19) are transformed into:

$$f''' + ff'' = \xi(f'g' - f''g), \tag{2.23}$$

$$(\frac{1}{Pr})\theta'' + f\theta' - 2\lambda\theta f' = \xi(f'\phi - \theta' g), \tag{2.24}$$

with

$$f + \xi = -\xi g, \quad f'(\xi,0) = \theta(\xi,\infty) = 0, \quad f'(\xi,\infty) = \theta(\xi,0) = 1, \tag{2.25}$$

In order to obtain auxiliary equations for g and ϕ, the equations (2.23) - (2.25) are differentiated with respect to ξ.

$$g''' + fg'' + f''g = \xi[\frac{\partial}{\partial \xi}(f'g' - f''g)] + f'g' - f''g, \tag{2.26}$$

$$(\frac{1}{Pr})\phi'' + f\phi' + \theta' g - 2\lambda g'\theta - 2\lambda\phi f' = \xi[\frac{\partial}{\partial\xi}(f'\phi - \theta' g)] + f'\phi - \theta' g, \tag{2.27}$$

with

$$2g + 1 = -\xi\frac{\partial g}{\partial\xi}, \quad g'(\xi,0) = g'(\xi,\infty) = \phi(\xi,0) = \phi(\xi,\infty) = 0. \tag{2.28}$$

Removing $\xi[\frac{\partial}{\partial\xi}(f'g' - f''g)]$ and $\xi[\frac{\partial}{\partial\xi}(f'\phi - \theta' g)]$, as well as deleting the partial derivatives $\frac{\partial g}{\partial\xi}$ and $\frac{\partial\phi}{\partial\xi}$.

The whole set of equations at the second level can be formulated as:

$$f''' + ff'' = \xi(f'g' - f''g), \tag{2.29}$$

$$g''' + 2f''g - f'g' + fg'' = 0, \tag{2.30}$$

$$(\frac{1}{Pr})\theta'' + f\theta' - 2\lambda\theta f' = \xi(f'\phi - \theta' g), \tag{2.31}$$

$$(\frac{1}{Pr})\phi'' - f'\phi(1 + 2\lambda) + f\phi' + 2g\theta' - 2\lambda g'\theta = 0, \tag{2.32}$$

with

$$f(\xi,0) = -\frac{1}{2}\xi, \quad g(\xi,0) = -\frac{1}{2}, \quad f'(\xi,0) = g'(\xi,0) = \phi(\xi,0) = 0, \quad \theta(\xi,0) = 1,$$
$$f'(\xi,\infty) = 1, \quad g'(\xi,\infty) = \theta(\xi,\infty) = \phi(\xi,\infty) = 0. \tag{2.33}$$

3rd Level of Truncation

At this level, the governing equations (Eqs. 2.17 and 2.18) are preserved without any approximations. The equations are then differentiated twice with respect to ξ, and two new variables named h and χ are introduced.

$$h''' + fh'' + 4gg'' - 2f'h' - 2g'^2 + 3f''h = \xi\left[\frac{\partial^2}{\partial\xi^2}(f'g' - f''g)\right], \tag{2.34}$$

$$(\frac{1}{Pr})\chi'' + f\chi' - f'\chi(2 + 2\lambda) - \phi g'(2 + 4\lambda) + 4g\phi' - 2\lambda h'\theta + 3\theta' h =$$
$$\xi\left[\frac{\partial^2}{\partial\xi^2}(f'\phi - \theta' g)\right]. \tag{2.35}$$

Deleting the terms $\xi[\frac{\partial^2}{\partial\xi^2}(f'g' - f''g)]$, $\xi[\frac{\partial^2}{\partial\xi^2}(f'\phi - \theta' g)]$, and discarding the partial derivatives $\frac{\partial h}{\partial\xi}$ and $\frac{\partial\chi}{\partial\xi}$. The whole set of equations at the third level can be formulated as:

$$f''' + ff'' = \xi(f'g' - f''g), \tag{2.36}$$

$$g''' + 2f''g - f'g' + fg'' = \xi(f'h' + g'^2 - f''h - gg''), \tag{2.37}$$

$$(\frac{1}{Pr})\theta'' + f\theta' - 2\lambda\theta f' = \xi(f'\phi - \theta' g), \tag{2.38}$$

$$(\frac{1}{Pr})\phi'' - f'\phi(1 + 2\lambda) + f\phi' + 2g\theta' - 2\lambda g'\theta = \xi(g'\phi + f'\chi - \phi' g - \theta' h), \tag{2.39}$$

$$h''' + fh'' + 4gg'' - 2f'h' - 2g'^2 + 3f''h = 0, \tag{2.40}$$

$$(\frac{1}{Pr})\chi'' + f\chi' - f'\chi(2+2\lambda) - \phi g'(2+4\lambda) + 4g\phi' - 2\lambda h'\theta + 3\theta' h = 0, \quad (2.41)$$

with

$$f(\xi,0) = -\frac{1}{2}\xi, \quad g(\xi,0) = -\frac{1}{2},$$
$$f'(\xi,0) = g'(\xi,0) = \phi(\xi,0) = h(\xi,0) = h'(\xi,0) = \chi(\xi,0) = 0, \quad \theta(\xi,0) = 1,$$
$$f'(\xi,\infty) = 1, \quad g'(\xi,\infty) = \theta(\xi,\infty) = \phi(\xi,\infty) = h'(\xi,\infty) = \chi(\xi,\infty) = 0. \quad (2.42)$$

2.0.2 Transverse Curvature

When fluid flows along the surface of a cylinder in a direction perpendicular to its axis, it creates what is known as a boundary layer. The presence of transverse curvature on the cylinder's surface results in a velocity field that lacks similarity. More precisely, the flow of fluid along the surface of a circular cylinder with a radius of R positioned in a uniform free stream is influenced by the transverse curvature in a dissimilar manner. The applicable equations for the flow of the boundary layer in cylindrical coordinates (x and r) are as follows:

$$\frac{\partial}{\partial x}(ru) + \frac{\partial}{\partial r}(rv) = 0, \quad (2.43)$$

$$uu_x + vu_r = (\frac{\nu}{r})[\frac{\partial}{\partial r}(ru_r)], \quad (2.44)$$

$$uT_x + vT_r = (\frac{\alpha}{r})[\frac{\partial}{\partial r}(rT_r)]. \quad (2.45)$$

Seban and Bond proposed a method of transformation that can be used to simplify a process

$$\xi = (\frac{4}{R})\sqrt{\frac{\nu x}{U_\infty}}, \quad \eta = [\frac{(r^2 - R^2)}{4R}]\sqrt{\frac{U_\infty}{\nu x}}, \quad (2.46)$$

$$f(\xi,\eta) = \frac{\psi}{R}\sqrt{\nu x U_\infty}, \quad \theta(\xi,\eta) = \frac{T - T_\infty}{T_w - T_\infty}. \quad (2.47)$$

Eq. (2.44) and (2.45) becomes

$$(1+\xi\eta)\frac{\partial^3 f}{\partial\eta^3} + f\frac{\partial^2 f}{\partial\eta^2} + \xi\frac{\partial^2 f}{\partial\eta^2} = \xi(\frac{\partial f}{\partial\eta}\frac{\partial^2 f}{\partial\eta\partial\xi} - \frac{\partial^2 f}{\partial\eta^2}\frac{\partial f}{\partial\xi}), \quad (2.48)$$

$$(1+\xi\eta)\frac{\partial^2\theta}{\partial\eta^2} + (\xi + Prf)\frac{\partial\theta}{\partial\eta} = Pr\xi(\frac{\partial f}{\partial\eta}\frac{\partial\theta}{\partial\xi} - \frac{\partial\theta}{\partial\eta}\frac{\partial f}{\partial\xi}), \quad (2.49)$$

with

$$f(\xi,0) = \frac{\partial f}{\partial\eta}(\xi,0) = \theta(\xi,\infty) = 0, \quad \frac{\partial f}{\partial\eta}(\xi,\infty) = 2, \quad \theta(\xi,0) = 1. \quad (2.50)$$

Equations (2.48)-(2.50) can be restated as:

$$(1+\xi\eta)f''' + ff'' + \xi f'' = \xi(f'g' - f''g), \quad (2.51)$$

$$(1+\xi\eta)\theta'' + (\xi + Prf)\theta' = Pr\xi(f'\phi - \theta' g), \quad (2.52)$$

and

$$f(\xi,0) = f'(\xi,0) = \theta(\xi,\infty) = 0, \quad f'(\xi,\infty) = 2, \quad \theta(\xi,0) = 1. \quad (2.53)$$

1^{st} Level of Truncation (Local Similarity)

At this level, the RHS's of equations (2.51) and (2.52) can be treated as negligible. This simplification results in the boundary-layer equations and conditions being reduced to the following:

$$(1+\xi\eta)f''' + ff'' + \xi f'' = 0, \tag{2.54}$$

$$(1+\xi\eta)\theta'' + (\xi + Prf)\theta' = 0, \tag{2.55}$$

and

$$f(\xi,0) = f'(\xi,0) = \theta(\xi,\infty) = 0, \quad f'(\xi,\infty) = 2, \quad \theta(\xi,0) = 1. \tag{2.56}$$

2^{nd} Level of Truncation (Local Non-Similarity)

This level preserves the governing equations for f and θ, as given in Eqs. 2.51 and 2.52, without any approximations. Two new variables, $\frac{\partial f}{\partial \xi} = g$ and $\frac{\partial \theta}{\partial \xi} = \phi$, are introduced. By incorporating these variables, equations (2.51) through (2.53) can be expressed as:

$$(1+\xi\eta)f''' + ff'' + \xi f'' = \xi(f'g' - f''g), \tag{2.57}$$

$$(1+\xi\eta)g''' + \eta f''' + f''(2g+1) + g''(f+\xi) - f'g' = 0, \tag{2.58}$$

$$(1+\xi\eta)\theta'' + (\xi + Prf)\theta' = Pr\xi(f'\phi - \theta' g), \tag{2.59}$$

$$(1+\xi\eta)\phi'' + (\xi + Prf)\phi' - Prf'\phi + \eta\theta'' + (1+2Prg)\theta' = 0, \tag{2.60}$$

with

$$f(\xi,0) = f'(\xi,0) = g(\xi,0) = g'(\xi,0) = g'(\xi,\infty) = \theta(\xi,\infty) = \phi(\xi,0) = \phi(\xi,\infty) = 0,$$
$$f'(\xi,\infty) = 2, \quad \theta(\xi,0) = 1. \tag{2.61}$$

3^{rd} Level of Truncation

In the 3^{rd} level of truncation, the governing equations (Eqs. 2.51 and 2.52) are subjected to double differentiation with respect to ξ without any approximations. Two new variables, h and χ, are also introduced at this level.

Deleting the terms $\xi[\frac{\partial^2}{\partial \xi^2}(f'g' - f''g)]$, $\xi[\frac{\partial^2}{\partial \xi^2}(f'\phi - \theta' g)]$, and discarding the partial derivatives $\frac{\partial h}{\partial \xi}$ and $\frac{\partial \chi}{\partial \xi}$.The whole set of equations at the third level can be formulated as:

$$(1+\xi\eta)f''' + ff'' + \xi f'' = \xi(f'g' - f''g), \tag{2.62}$$

$$(1+\xi\eta)g''' + \eta f''' + f''(2g+1) + g''(f+\xi) - f'g' = \xi(f'h' + g'^2 - f''h - gg''), \tag{2.63}$$

$$(1+\xi\eta)\theta'' + (\xi + Prf)\theta' = Pr\xi(f'\phi - \theta' g), \tag{2.64}$$

$$(1+\xi\eta)\phi'' + \eta\theta'' + (\xi + Prf)\phi' + \theta'(1+2Prg) - Prf'\phi = \xi(g'\phi + f'\chi - \phi' g - \theta' h), \tag{2.65}$$

$$(1+\xi\eta)h''' + 2\eta g''' + g''(4g+2) + h''(f+\xi) + 3f''h - 2f'h' - 2g'^2 = 0, \tag{2.66}$$

$$(1+\xi\eta)\chi'' + 2\eta\phi'' + 3Pr\theta' h + \phi'(4Prg+2) + \chi'(\xi + Prf)$$
$$- 2Prf'\chi - 2Pr\phi g' = 0, \tag{2.67}$$

with

$$f(\xi,0) = 0, \quad g(\xi,0) = 0,$$
$$f'(\xi,0) = g'(\xi,0) = \phi(\xi,0) = h(\xi,0) = h'(\xi,0) = \chi(\xi,0) = 0, \quad \theta(\xi,0) = 1,$$
$$f'(\xi,\infty) = 2, \quad g'(\xi,\infty) = \theta(\xi,\infty) = \phi(\xi,\infty) = h'(\xi,\infty) = \chi(\xi,\infty) = 0. \tag{2.68}$$

2.0.3 Stream-wise Variations of Free-stream velocity

This section talks about how changes in the speed of a fluid as it flows in a particular direction (called "stream-wise direction") can affect the way the fluid behaves. When these changes follow a pattern where the speed is proportional to x raised to a power, the boundary layers of the fluid (the layers of fluid closest to the surface it flows over) have similar characteristics at different points along the stream-wise direction.

However, if the changes in speed follow a different pattern, the boundary layers become non-similar, which means they have different characteristics at different points along the stream-wise direction. This also affects the way heat is transferred between the fluid and the surface it flows over.

This section then goes on to describe an analysis of these non-similar boundary layers, where the way the temperature changes on the surface is restricted to a specific mathematical form called a power-law. The equations used to analyze these boundary layers are adjusted to take into account the changes in speed along the stream-wise direction.

$$uu_x + vu_y = U(\frac{\mathrm{d}U}{\mathrm{d}x}) + \nu u_{yy}, \tag{2.69}$$

$$uT_x + vT_y = \nu T_{yy}, \tag{2.70}$$

with

$$u = v = 0 \quad at \quad y = 0, \quad T = T_w; \quad u \to U(x), \quad T \to T_\infty \quad as \quad y \to \infty. \tag{2.71}$$

To develop a solution method, the problem must be transformed from the x, y coordinate system to the ξ, η system

$$\eta = y\sqrt{\frac{U}{2\nu x}}, \quad \xi = \frac{x}{L}, \tag{2.72}$$

and

$$f(\xi,\eta) = \frac{\psi}{\sqrt{2\nu x U}}, \quad \theta(\xi,\eta) = \frac{T - T_\infty}{T_w - T_\infty}. \tag{2.73}$$

The system of equations (2.69)-(2.71) can be solved by introducing a new function called the stream function $\psi(\xi,\eta)$, which relates to the velocity components as follows:

$$u = \frac{\partial\psi}{\partial y} \quad and \quad v = \frac{-\partial\psi}{\partial x}, \tag{2.74}$$

$$u = Uf'(\xi,\eta), \tag{2.75}$$

$$v = \sqrt{\frac{U\nu}{2x}}(\eta f' - f) - \frac{\sqrt{2\nu x U}}{L}\frac{\partial f}{\partial \xi}. \tag{2.76}$$

Equations (2.69) and (2.70) will be modified after implementing these transformations as

$$\frac{\partial^3 f}{\partial\eta^3} + f\frac{\partial^2 f}{\partial\eta^2} + \beta(1 - (\frac{\partial f}{\partial\eta})^2) = 2\xi(\frac{\partial f}{\partial\eta}\frac{\partial^2 f}{\partial\eta\partial\xi} - \frac{\partial^2 f}{\partial\eta^2}\frac{\partial f}{\partial\xi}), \tag{2.77}$$

$$(\frac{1}{Pr})\frac{\partial^2\theta}{\partial\eta^2} + (\beta+1)f\frac{\partial\theta}{\partial\eta} - 2\lambda\frac{\partial f}{\partial\eta}\theta = 2\xi(\frac{\partial f}{\partial\eta}\frac{\partial\theta}{\partial\xi} - \frac{\partial\theta}{\partial\eta}\frac{\partial f}{\partial\xi}), \tag{2.78}$$

with

$$f(\xi,0) = f'(\xi,0) = \theta(\xi,\infty) = 0, \quad f'(\xi,\infty) = 1, \quad \theta(\xi,0) = 1. \tag{2.79}$$

Equations (2.77)-(2.79) can be restated as:

$$f''' + ff'' + \beta(1 - ff'^2) = 2\xi(f'g' - f''g), \tag{2.80}$$

$$(\frac{1}{Pr})\theta'' + (\beta+1)f\theta' - 2\lambda f'\theta = 2\xi(f'\phi - \theta' g), \tag{2.81}$$

where,

$$\beta = (\frac{2x}{U})(\frac{\mathrm{d}U}{\mathrm{d}x}).$$

First Level of Truncation (Local Similarity)

At this level , the RHS's of equations (2.80) and (2.81) can be considered negligible and treated as zero. Consequently, the boundary-layer equations and conditions can be simplified as

$$f''' + ff'' + \beta(1 - ff'^2) = 0, \tag{2.82}$$

$$(\frac{1}{Pr})\theta'' + (\beta+1)f\theta' - 2\lambda f'\theta = 0, \tag{2.83}$$

and

$$f(\xi,0) = f'(\xi,0) = \theta(\xi,\infty) = 0, \quad f'(\xi,\infty) = 1, \quad \theta(\xi,0) = 1. \tag{2.84}$$

Local Non-Similarity

This level preserves the governing equations for f and θ, as given in Eqs. (2.80) and (2.81), without any approximations. Two new variables, $\frac{\partial f}{\partial\xi} = g$ and $\frac{\partial\theta}{\partial\xi} = \phi$, are introduced. By incorporating these variables, equations (2.80) through (2.81) can be expressed as:

$$f''' + ff'' + \beta(1 - f'^2) = 2\xi(f'g' - f''g), \tag{2.85}$$

$$g''' + fg'' + 3f''g - 2f'g'(\beta+1) + \frac{\mathrm{d}\beta}{\mathrm{d}\xi}(1 - f'^2) = 0, \tag{2.86}$$

$$(\frac{1}{Pr})\theta'' + (\beta+1)f\theta' - 2\lambda f'\theta = 2\xi(f'\phi - \theta' g), \tag{2.87}$$

$$(\frac{1}{Pr})\phi'' + \theta' g + \beta f\phi' + \frac{\mathrm{d}\beta}{\mathrm{d}\xi}(f\theta') - 2f'\phi(1+\lambda) - 2\lambda\theta g' = 0, \tag{2.88}$$

with

$$f(\xi,0) = f'(\xi,0) = g(\xi,0) = g'(\xi,0) = g'(\xi,\infty) = \theta(\xi,\infty) = \phi(\xi,0) = \phi(\xi,\infty) = 0,$$
$$f'(\xi,\infty) = \theta(\xi,0) = 1, \tag{2.89}$$

for specific value of $U(x)$

$$U(x) = U_\infty e^{\frac{\omega x}{L}}, \quad \beta = 2\omega\xi, \quad \frac{\mathrm{d}\beta}{\mathrm{d}\xi} = 2\omega.$$

2.0.4 Stream-wise Variations of Surface Temperature

This section focuses on the non-similarity of thermal boundary layers caused by variations in surface temperature along the streamwise direction. Only power-law variations in surface temperature allow for similarity. The velocity boundary layer is assumed to have a self-similar structure, with the free-stream velocity represented as $U \sim x^{\omega}$. The equations governing the streamwise variations of the thermal boundary layer are as follows:

$$uu_x + vu_y = U(\frac{\mathrm{d}U}{\mathrm{d}x}) + \nu u_{yy}, \tag{2.90}$$

$$uT_x + vT_y = \alpha T_{yy}, \tag{2.91}$$

with,

$$u = v = 0 \quad at \quad y = 0, \quad T = T_w; \quad u \to U(x), \quad T \to T_\infty \quad as \quad y \to \infty. \tag{2.92}$$

Suitable velocity similarity variables are:

$$\eta = y\sqrt{\frac{U_\infty}{2\nu x}}, \quad f(\eta) = \frac{\psi}{\sqrt{2\nu x U}}, \tag{2.93}$$

$$u = U_o x^{\omega} f', \tag{2.94}$$

$$v = \left[-(\frac{\omega+1}{2})f - \eta(\frac{\omega-1}{2})f'\right]\sqrt{2\nu U_o x^{\omega-1}}. \tag{2.95}$$

Using Eq. (2.92)-(2.95) in (2.90) we have,

$$f''' + (\omega+1)ff'' - 2\omega f'^2 = 0, \tag{2.96}$$

The function f is clearly a function of only η. This is evident from the fact that the function definition does not include any other variables.

$$\theta(\xi,\eta) = \frac{T - T_\infty}{T_w - T_\infty}, \quad \xi = \frac{x}{L}, \tag{2.97}$$

$$\frac{\partial T}{\partial x} = \theta\frac{dT_w}{dx} + \frac{T_w - T_\infty}{L}\frac{\partial\theta}{\partial\xi} + \left[\frac{(T_w - T_\infty)(\omega-1)}{2x}\eta\theta'\right], \tag{2.98}$$

$$\frac{\partial T}{\partial y} = (T_w - T_\infty)\left[\theta'\sqrt{\frac{U_o x^{\omega-1}}{2\nu}}\right], \tag{2.99}$$

$$\frac{\partial^2 T}{\partial y^2} = \frac{(T_w - T_\infty)(U_o x^{\omega-1})}{2\nu}\theta'', \tag{2.100}$$

Using Eq. (2.93), (2.94), (2.96), (2.97), (2.98), and (2.99) in (2.91)
$\Rightarrow$

$$U_o x^{\omega}\frac{dT_w}{dx}f'\theta + \xi U_o x^{\omega-1}(T_w - T_\infty)\frac{\partial\theta}{\partial\xi}f' - \frac{(T_w - T_\infty)}{2}U_o(\omega+1)x^{\omega-1}f\theta'$$
$$= (T_w - T_\infty)\frac{U_o x^{\omega-1}}{2\nu}\theta'', \tag{2.101}$$

$$(\frac{1}{Pr})\theta'' - 2\Omega f'\theta + (\omega+1)f\theta' = 2\xi\frac{\partial\theta}{\partial\xi}f', \tag{2.102}$$

or,

$$(\frac{1}{Pr})\theta'' - 2\Omega f'\theta + (\omega+1)f\theta' = 2\xi\phi f', \tag{2.103}$$

where,

$$\Omega(\xi) = x\frac{(\frac{dT_w}{dx})}{(T_w - T_\infty)}$$

Local Similarity

In the 1^{st} level of truncation, the RHS's of equations (2.102) can be considered negligible and treated as zero. Consequently, the boundary-layer equations and conditions can be simplified as:

$$f''' + (\omega+1)ff'' - 2\omega f'^2 = 0, \tag{2.104}$$

$$(\frac{1}{Pr})\theta'' - 2\Omega f'\theta + (\omega+1)f\theta' = 0, \tag{2.105}$$

and

$$f(\xi,0) = f'(\xi,0) = \theta(\xi,\infty) = 0, \quad f'(\xi,\infty) = 1, \quad \theta(\xi,0) = 1. \tag{2.106}$$

Local Non-Similarity

The 2^{nd} level of truncation preserves the governing equations for f and θ, as given in Eqs. (2.96) and (2.103), without any approximations. New variable, $\frac{\partial\theta}{\partial\xi} = \phi$, is introduced. By incorporating this variable, equations (2.96) through (2.103) can be expressed as:

$$f''' + (\omega+1)ff'' - 2\omega f'^2 = 0, \tag{2.107}$$

$$(\frac{1}{Pr})\theta'' - 2\Omega f'\theta + (\omega+1)f\theta' = 2\xi\phi f', \tag{2.108}$$

$$(\frac{1}{Pr})\phi'' - (2+2\Omega)f'\phi + (\omega+1)f\phi' - 2(\frac{\mathrm{d}\Omega}{\mathrm{d}\xi})f'\theta = 0, \tag{2.109}$$

with,

$$f(\xi,0) = f'(\xi,0) = \theta(\xi,\infty) = \phi(\xi,0) = \phi(\xi,\infty) = 0,$$
$$f'(\xi,\infty) = \theta(\xi,0) = 1, \tag{2.110}$$

2.0.5 Results and Discussion

The review problem's physical aspects were analyzed using graphical methods. To solve the governing equations for temperature profiles, the BCP-4c method was employed. In Figure (2.1), the boundary temperature profiles for surface mass transfer are displayed for various values of ξ when $Pr = 0.7$ and $\alpha = 0$. It is evident that θ increases as ξ increases. Figure (2.2) presents different profiles of the local Nusselt number, including the local similarity, 2-equation model, and 3-equation model. Clearly, the 3-equation model yields the most accurate results compared to the other models. Figure (2.3) illustrates the boundary temperature profiles for transverse curvature at different values of ξ when $Pr = 0.7$. It can be observed that θ increases with increasing ξ. Similarly, Figure (2.4) demonstrates distinct profiles of the local Nusselt number, involving the local similarity, 2-equation model, and 3-equation model. The 3-equation model once again exhibits the most accurate results compared to the other models. Lastly, Figure

(2.6) showcases the effect of ξ on temperature profiles for a specific value of $U(x)$, where $U(x) = U_\infty e^{\frac{\omega x}{L}}$, with $\omega = 1$, $\Omega = \xi\lambda$, and $Pr = 0.7$.It can be observed that θ decreases with increasing ξ.

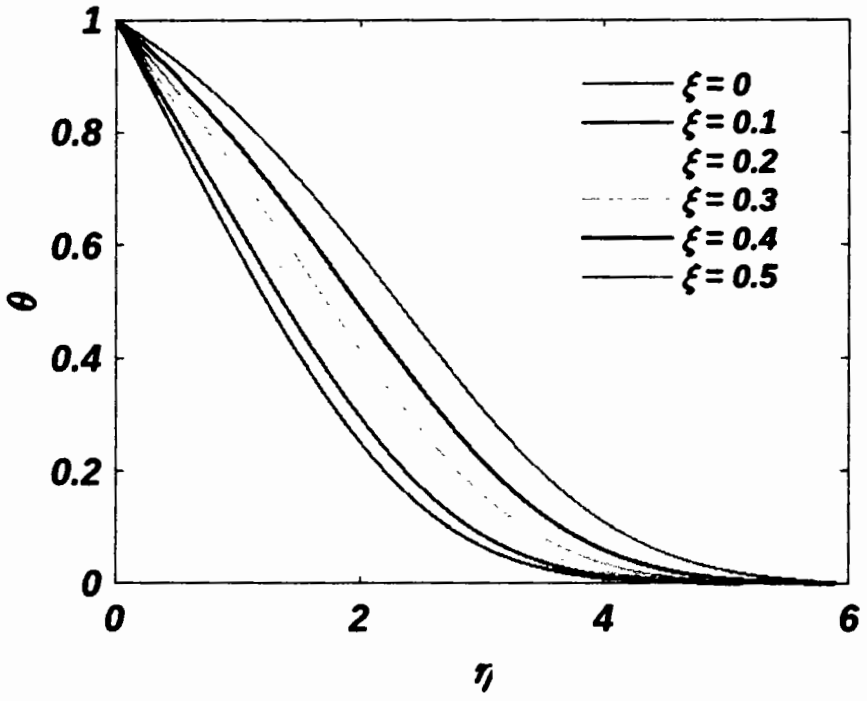

Figure 2.1: Temperature profiles in the boundary layer over a flat plate with uniform surface mass transfer

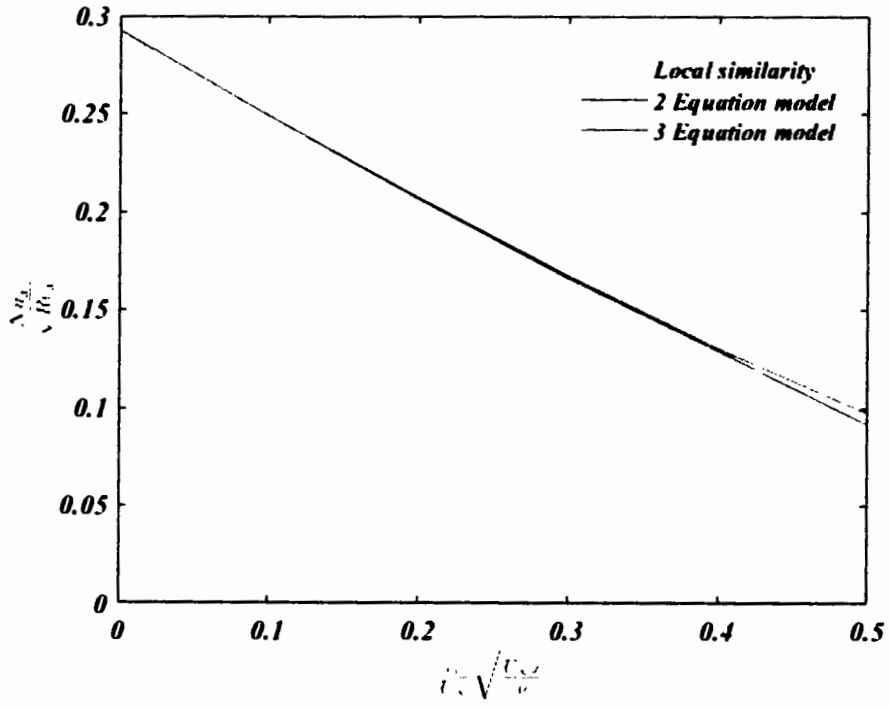

Figure 2.2: Local Nusselt Number for Local Similarity, 2 Equation, and 3 Equation Models

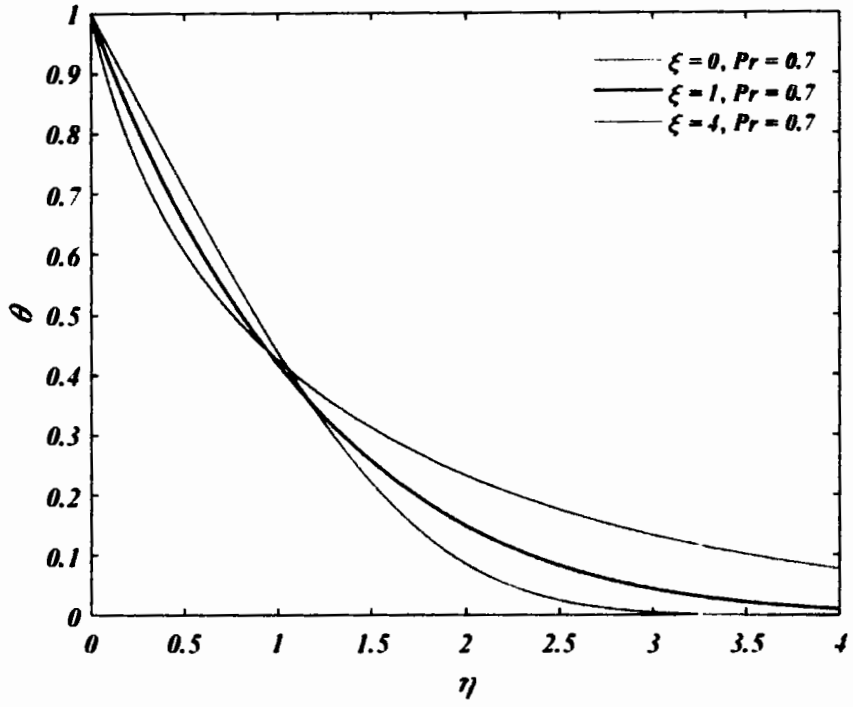

Figure 2.3: Temperature Profiles of the Boundary Layer: Cylinder in Longitudinal Flow

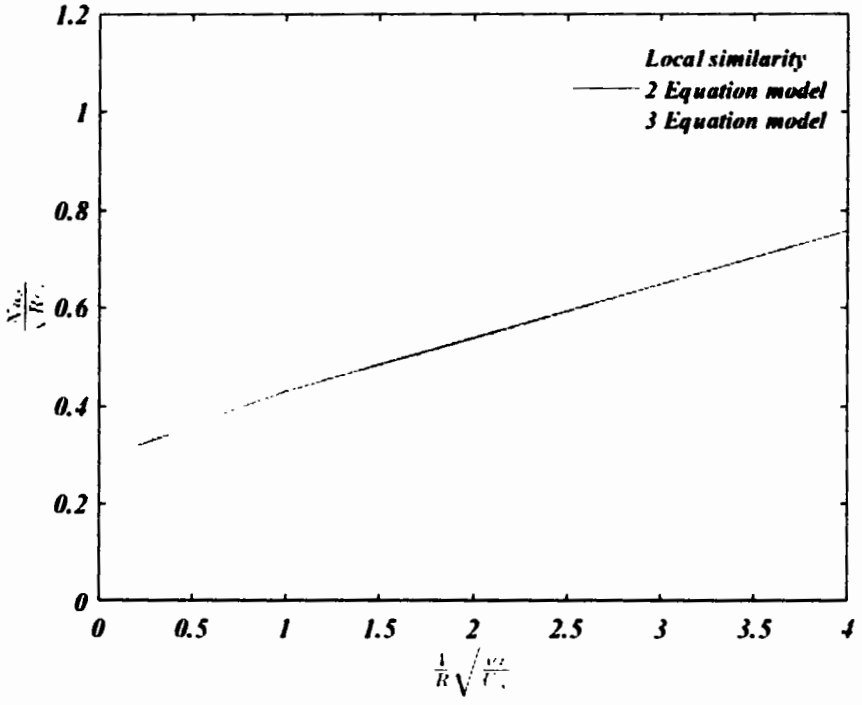

Figure 2.4: Local Nusselt Number for Local Similarity, 2 Equation, and 3 Equation Models

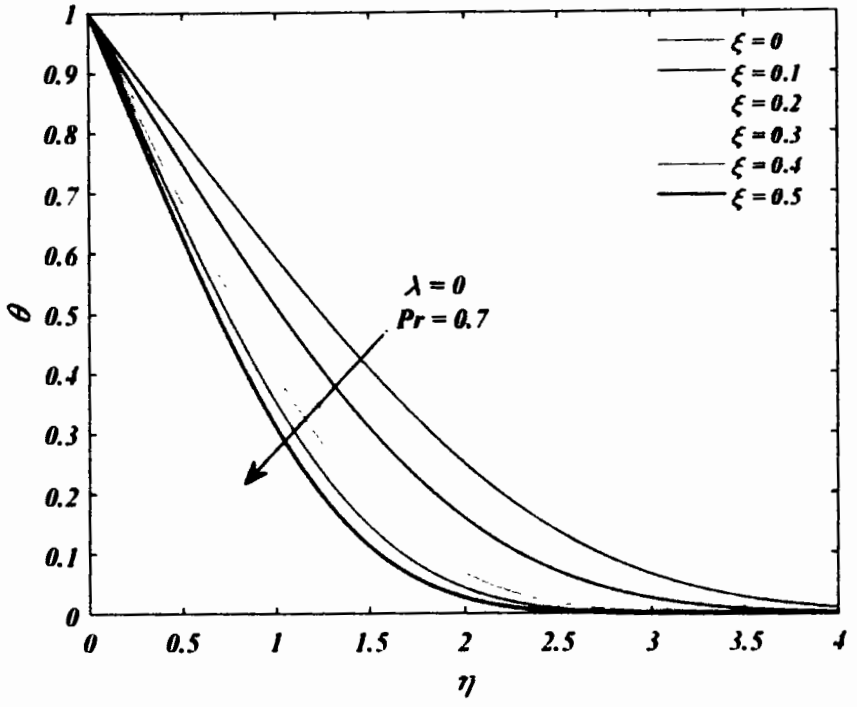

Figure 2.5: Temperature profiles in the boundary layer over a flat plate with streamwise variations of free-stream velocity

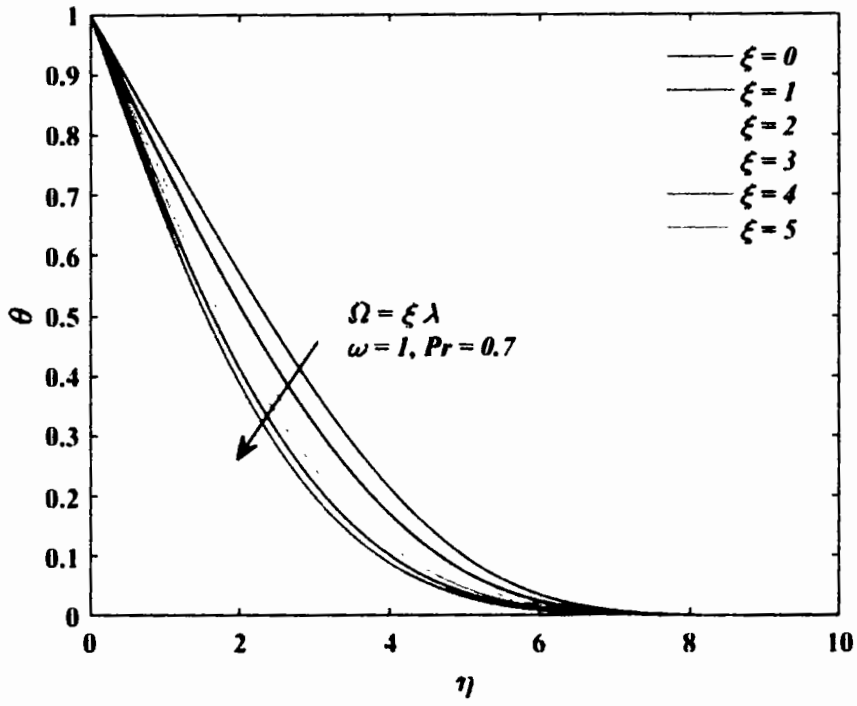

Figure 2.6: Effect of ξ on Temperature profiles when $\omega = 1$ and $Pr = 0.7$

2.0.6 Conclusion

In conclusion, this chapter discussed Local non-similarity thermal boundary-layer Solutions. The results of local similarity (1st truncation), 2nd truncation, and third truncation were presented. Non-similarity arises due to surface mass transfer, transverse curvature, stream-wise variations of free-stream velocity, and stream-wise variations of surface temperature. Understanding these non-similar effects is essential for practical engineering and scientific applications. Future research can explore more complex scenarios and advanced numerical techniques to enhance boundary-layer understanding and optimize engineering designs.

TH-27642

Chapter 3

Local Non-similarity Solution Method for the Flow of a Williamson Fluid over a Stretching Sheet

In this chapter, the local non-similarity solution method is employed to analyze the two-dimensional flow of the Williamson fluid. This method is used to transform governing partial differential equations of the Williamson fluid into an ordinary differential equation. This transformed equation is then solved numerically by the bvp4c method. The results of the investigation are presented in both tabular and graphical formats. These representations provide a comprehensive view of fluid behavior and a deeper understanding of the flow characteristics. By examining the numerical outcomes, valuable insights can be gained into the local properties of the Williamson fluid and its impact on the two-dimensional flow.

3.0.1 Mathematical model

Let us examine the steady, two-dimensional flow of an incompressible boundary layer of Williamson fluid over a flat plate [12]. The equations governing this analysis can be expressed as:

$$u_x + v_y = 0, \tag{3.1}$$

In the absence of body forces, the conservation of linear momentum is,

$$\rho \frac{d\mathbf{V}}{dt} = \nabla \cdot \mathbf{S}, \tag{3.2}$$

$$\frac{d\mathbf{V}}{dt} = \frac{\partial \mathbf{V}}{\partial t} + (\mathbf{V} \cdot \nabla)\mathbf{V}. \tag{3.3}$$

For steady flow, $\frac{\partial \mathbf{V}}{\partial t} = 0$, (3.3) becomes:

$$\frac{dV}{dt} = (\mathbf{V} \cdot \nabla)\mathbf{V} \tag{3.4}$$

Now (3.2) $\Longrightarrow$

$$\rho(uu_x + vu_y) = (\nabla.\mathbf{S})_x, \tag{3.5}$$

$$\rho(uv_x + vv_y) = (\nabla.\mathbf{S})_y, \tag{3.6}$$

where,

$$\mathbf{S} = -p\mathbf{I} + \boldsymbol{\tau}, \tag{3.7}$$

and,

$$\boldsymbol{\tau} = \left[\mu_\infty + \frac{(\mu_0 - \mu_\infty)}{1 + \Gamma|\dot{\gamma}|}\right] \mathbf{A}_1. \tag{3.8}$$

Here, the Rivlin Ericksen tensor is denoted by $\mathbf{A}_1$ is Rivlin Ericksen tensor, the pressure by p, the extra stress tensor by τ, the infinite shear rate viscosity by μ_∞ is the infinite shear rate viscosity, the zero shear rate viscosity by μ_0, the time constant by Γ, the identity tensor by $\overline{I}$ and shear rate $\dot{\gamma}$ is defined as:

$$\dot{\gamma} = \sqrt{\frac{1}{2}\text{trace}(\mathbf{A_1}^2)}, \tag{3.9}$$

where,

$$\mathbf{A}_1 = \nabla\mathbf{V} + (\nabla\mathbf{V})^T, \tag{3.10}$$

$$\nabla\mathbf{V} = \begin{bmatrix} u_x & u_y & 0 \\ v_x & v_y & 0 \\ 0 & 0 & 0 \end{bmatrix}, \tag{3.11}$$

$$(\nabla\mathbf{V})^T = \begin{bmatrix} u_x & v_x & 0 \\ u_y & v_y & 0 \\ 0 & 0 & 0 \end{bmatrix}, \tag{3.12}$$

$$\mathbf{A_1} = \begin{bmatrix} 2u_x & v_x + u_y & 0 \\ v_x + u_y & 2v_y & 0 \\ 0 & 0 & 0 \end{bmatrix}, \tag{3.13}$$

$$\mathbf{A_1}^2 = \begin{bmatrix} 4u_x^2 + (v_x + u_y)^2 & (v_x + u_y)(2u_x) + (v_x + u_y)(2v_y) & 0 \\ (2u_x)(v_x + u_y) + (v_x + u_y)(2v_y) & 4v_y^2 + (v_x + u_y)^2 & 0 \\ 0 & 0 & 0 \end{bmatrix}, \tag{3.14}$$

$$trace(\mathbf{A_1}^2) = 2[2(u_x^2 + v_y^2) + (v_x + u_y)^2], \tag{3.15}$$

$$\frac{trace(\mathbf{A_1}^2)}{2} = [2(u_x^2 + v_y^2) + (v_x + u_y)^2], \tag{3.16}$$

$$|\dot{\gamma}| = \sqrt{\frac{trace(\mathbf{A_1}^2)}{2}} = (2u_x^2 + (v_x + u_y)^2 + 2v_y^2)^{\frac{1}{2}}. \tag{3.17}$$

Consider, $\mu_\infty = 0$
Now, Eq. (3.8) $\Longrightarrow$

$$\boldsymbol{\tau} = \left[\frac{\mu_0}{1 + \Gamma|\dot{\gamma}|}\right] \mathbf{A_1}, \tag{3.18}$$

$$\begin{bmatrix} \tau_{xx} & \tau_{xy} & \tau_{xz} \\ \tau_{yx} & \tau_{yy} & \tau_{yz} \\ \tau_{zx} & \tau_{zy} & \tau_{zz} \end{bmatrix} = \left[\frac{\mu_0}{1 + \Gamma|\dot{\gamma}|}\right] \begin{bmatrix} 2u_x & v_x + u_y & 0 \\ v_x + u_y & 2v_y & 0 \\ 0 & 0 & 0 \end{bmatrix}, \tag{3.19}$$

$$\tau_{xx} = \left[\frac{2\mu_0 u_x}{1+\Gamma|\dot{\gamma}|}\right], \tag{3.20}$$

$$\tau_{xy} = \left[\frac{\mu_0(v_x+u_y)}{1+\Gamma|\dot{\gamma}|}\right], \tag{3.21}$$

$$\tau_{xz} = 0, \tag{3.22}$$

$$\tau_{yx} = \left[\frac{\mu_0(v_x+u_y)}{1+\Gamma|\dot{\gamma}|}\right], \tag{3.23}$$

$$\tau_{yy} = \left[\frac{2\mu_0 v_y}{1+\Gamma|\dot{\gamma}|}\right], \tag{3.24}$$

$$\tau_{yz} = 0, \tag{3.25}$$

$$\tau_{zx} = 0, \tag{3.26}$$

$$\tau_{zy} = 0, \tag{3.27}$$

$$\tau_{zz} = 0, \tag{3.28}$$

Now, Eq.(3.7) $\Longrightarrow$

$$\begin{bmatrix} S_{xx} & S_{xy} & S_{xz} \\ S_{yx} & S_{yy} & S_{yz} \\ S_{zx} & S_{zy} & S_{zz} \end{bmatrix} = \begin{bmatrix} -p & 0 & 0 \\ 0 & -p & 0 \\ 0 & 0 & -p \end{bmatrix} + \begin{bmatrix} \left[\frac{2\mu_0 u_x}{1+\Gamma|\dot{\gamma}|}\right] & \left[\frac{\mu_0(v_x+u_y)}{1+\Gamma|\dot{\gamma}|}\right] & 0 \\ \left[\frac{\mu_0(v_x+u_y)}{1+\Gamma|\dot{\gamma}|}\right] & \left[\frac{2\mu_0 v_y}{1+\Gamma|\dot{\gamma}|}\right] & 0 \\ 0 & 0 & 0 \end{bmatrix}, \tag{3.29}$$

$$S_{xx} = -p + \left[\frac{2\mu_0 u_x}{1+\Gamma|\dot{\gamma}|}\right], \tag{3.30}$$

$$S_{xy} = \left[\frac{\mu_0(v_x+u_y)}{1+\Gamma|\dot{\gamma}|}\right], \tag{3.31}$$

$$S_{xz} = 0, \tag{3.32}$$

$$S_{yx} = \left[\frac{\mu_0(v_x+u_y)}{1+\Gamma|\dot{\gamma}|}\right], \tag{3.33}$$

$$S_{yy} = -p + \left[\frac{2\mu_0 v_y}{1+\Gamma|\dot{\gamma}|}\right], \tag{3.34}$$

$$S_{yz} = 0, \tag{3.35}$$

$$S_{zx} = 0, \tag{3.36}$$

$$S_{zy} = 0, \tag{3.37}$$

$$S_{zz} = -p, \tag{3.38}$$

Now, Eq. (3.5) and (3.6) $\Longrightarrow$

$$\rho(uu_x + vu_y) = \frac{\partial S_{xx}}{\partial x} + \frac{\partial S_{xy}}{\partial y},$$

$$= \frac{\partial(-p + \left[\frac{2\mu_0 u_x}{1+\Gamma|\dot{\gamma}|}\right])}{\partial x} + \frac{\partial(\left[\frac{\mu_0(v_x+u_y)}{1+\Gamma|\dot{\gamma}|}\right])}{\partial y}, \tag{3.39}$$

$$\rho(uv_x + vv_y) = \frac{\partial S_{yx}}{\partial x} + \frac{\partial S_{yy}}{\partial y},$$

$$= \frac{\partial(\left[\frac{\mu_0(v_x+u_y)}{1+\Gamma|\dot{\gamma}|}\right])}{\partial x} + \frac{\partial(-p+\left[\frac{2\mu_0 v_y}{1+\Gamma|\dot{\gamma}|}\right])}{\partial y}. \tag{3.40}$$

Where, $|\dot{\gamma}| = (2u_x^2 + (v_x+u_y)^2 + 2v_y^2)^{\frac{1}{2}}$. Applying boundary layer approximation, $\Longrightarrow$

$$\rho(uu_x + vu_y) = \nu\frac{\partial}{\partial y}\left[\frac{u_y}{1+\Gamma|\dot{\gamma}|}\right]. \tag{3.41}$$

The flow behavior of a Williamson fluid is described by the following governing equations:

$$u_x + v_y = 0, \tag{3.42}$$

$$uu_x + vu_y = \nu\left[\frac{\partial}{\partial y}\left(\frac{u_y}{1+\Gamma|\dot{\gamma}|}\right)\right]. \tag{3.43}$$

,

$$uT_x + vT_y = \alpha T_{yy}. \tag{3.44}$$

The boundary conditions for the velocity and temperature fields are specified as follows:

$$\begin{cases} u = U_w = ax,\ v = 0,\ T = T_w & at \quad y = 0 \\ u = 0,\ T = T_\infty & as \quad y \to \infty \end{cases}. \tag{3.45}$$

To develop a solution method, the problem must be transformed from the x, y coordinate system to the ξ, η system [16]. Introducing the following parameters

$$\xi = \sqrt{\frac{a}{\nu}}x, \quad \eta = \sqrt{\frac{a}{\nu}}y, \tag{3.46}$$

$$u = axp'(\xi,\eta), \quad v = -\sqrt{a\nu}(p + \xi\frac{\partial p}{\partial \xi}), \tag{3.47}$$

$$\frac{\partial u}{\partial x} = \frac{\partial}{\partial x}\left[axp'(\xi,\eta)\right], \tag{3.48}$$

$$\frac{\partial u}{\partial x} = a\left[x(\frac{\partial p'}{\partial \xi}\frac{\partial \xi}{\partial x} + \frac{\partial p'}{\partial \eta}\frac{\partial \eta}{\partial x}) + p'(\xi,\eta)\right], \tag{3.49}$$

$$\frac{\partial u}{\partial x} = a\left[\xi\frac{\partial p'}{\partial \xi} + p'\right], \tag{3.50}$$

$$u\frac{\partial u}{\partial x} = a^2x\left[\xi\frac{\partial p'}{\partial \xi}p' + p'^2\right], \tag{3.51}$$

$$\frac{\partial u}{\partial y} = \frac{\partial}{\partial y}\left[axp'(\xi,\eta)\right], \tag{3.52}$$

$$\frac{\partial u}{\partial y} = ax(\frac{\partial p'}{\partial \xi}\frac{\partial \xi}{\partial y} + \frac{\partial p'}{\partial \eta}\frac{\partial \eta}{\partial y}), \tag{3.53}$$

$$\frac{\partial u}{\partial y} = a\xi p'', \tag{3.54}$$

$$v\frac{\partial u}{\partial x} = -a^2 x\left[pp'' + \xi p''\frac{\partial p}{\partial \xi}\right], \tag{3.55}$$

$$\frac{\partial^2 u}{\partial y^2} = \frac{a^2 x}{\nu}p''', \tag{3.56}$$

For simplification taking positive value of $|\dot{\gamma}|$, then Eq.(3.43) $\Longrightarrow$

$$uu_x + vu_y = \nu\frac{\partial}{\partial y}\left[\frac{u_y}{1-\Gamma\dot{\gamma}}\right] \tag{3.57}$$

$$a^2 x\left[\xi\frac{\partial p'}{\partial \xi}p' + p'^2 - pp'' - \xi p''\frac{\partial p}{\partial \xi}\right] = \nu\frac{\partial}{\partial y}\left[\frac{a\sqrt{\frac{a}{\nu}}xp''(\xi,\eta)}{1-\Gamma(a\sqrt{\frac{a}{\nu}}xp''(\xi,\eta))}\right], \tag{3.58}$$

$$a^2 x\left[\xi\frac{\partial p'}{\partial \xi}p' + p'^2 - pp'' - \xi p''\frac{\partial p}{\partial \xi}\right] = \nu\frac{a^2 x}{\nu}\left[\frac{p'''}{(1-\Gamma(a\xi p''))^2}\right], \tag{3.59}$$

$$a^2 x\left[\xi\frac{\partial p'}{\partial \xi}p' + p'^2 - pp'' - \xi p''\frac{\partial p}{\partial \xi}\right] = a^2 x\left[\frac{p'''}{(1-\Gamma(a\xi p''))^2}\right], \tag{3.60}$$

$\Longrightarrow$

$$\xi\frac{\partial p'}{\partial \xi}p' + p'^2 - pp'' - \xi p''\frac{\partial p}{\partial \xi} = \frac{p'''}{(1-\Gamma(a\xi p''))^2}, \tag{3.61}$$

or,

$$\xi\frac{\partial p'}{\partial \xi}p' + p'^2 - pp'' - \xi p''\frac{\partial p}{\partial \xi} = \frac{p'''}{(1-We\xi p'')^2}, \tag{3.62}$$

Here, We=Γa is the local Weissenberg number

$$p'''(1-We\xi p'')^{-2} - p'^2 + pp'' = \xi[\frac{\partial p'}{\partial \xi}p' - p''\frac{\partial p}{\partial \xi}], \tag{3.63}$$

with,

$$p(\xi,0) = -\xi\frac{\partial p}{\partial \xi}(\xi,0), \quad p'(\xi,0) = 1, \quad p'(\xi,\infty) = 0, \tag{3.64}$$

As,

$$\theta(\xi,\eta) = \frac{T-T_\infty}{T_w-T_\infty}, \tag{3.65}$$

$$T_x = (T_w-T_\infty)\sqrt{\frac{a}{\nu}}\left[\frac{\partial\theta}{\partial\xi}\right], \tag{3.66}$$

$$uT_x = \left[(T_w-T_\infty)\sqrt{\frac{a}{\nu}}\right](ax)(p'\frac{\partial\theta}{\partial\xi}), \tag{3.67}$$

$$T_y = \left[(T_w-T_\infty)\sqrt{\frac{a}{\nu}}\right]\theta', \tag{3.68}$$

$$vT_y = -a(T_w-T_\infty)\left[p\theta' + \xi\frac{\partial p}{\partial\xi}\theta'\right], \tag{3.69}$$

$$\frac{\partial^2 T}{\partial y^2} = \frac{a}{\nu}(T_w-T_\infty)\theta''. \tag{3.70}$$

Eq.(3.44) $\Longrightarrow$

$$(\frac{1}{Pr})\theta'' + p\theta' = \xi(p'\frac{\partial\theta}{\partial\xi} - \theta'\frac{\partial p}{\partial\xi}), \tag{3.71}$$

with,

$$\theta(\xi,0) = 1, \quad \theta(\xi,\infty) = 0, \tag{3.72}$$

$\Longrightarrow$

$$p'''(1-We\xi p'')^{-2} - p'^2 + pp'' = \xi\left[\frac{\partial p'}{\partial \xi}p' - p''\frac{\partial p}{\partial \xi}\right], \tag{3.73}$$

$$(\frac{1}{Pr})\theta'' + p\theta' = \xi(p'\frac{\partial \theta}{\partial \xi} - \theta'\frac{\partial p}{\partial \xi}), \tag{3.74}$$

with Boundary conditions,

$$p(\xi,0) = -\xi\frac{\partial p}{\partial \xi}(\xi,0), \quad p'(\xi,0) = 1, \quad p'(\xi,\infty) = 0, \tag{3.75}$$

$$\theta(\xi,0) = 1, \quad \theta(\xi,\infty) = 0, \tag{3.76}$$

1^{st} Level of Truncation (Local Similarity)

At this level , the right-hand terms of equations (3.73) and (3.74) can be considered negligible and treated as zero. Consequently, the boundary-layer equations and conditions can be simplified as

$$p''' - p'^2 + pp'' = 0, \tag{3.77}$$

$$(\frac{1}{Pr})\theta'' + p\theta' = 0, \tag{3.78}$$

and

$$p(\xi,0) = 0, \quad p'(\xi,0) = 1, \quad p'(\xi,\infty) = 0, \tag{3.79}$$

$$\theta(\xi,0) = 1, \quad \theta(\xi,\infty) = 0. \tag{3.80}$$

2^{nd} Level of Truncation

This level preserves the governing equations for p and ϕ, as given in Eqs. (3.77) and (3.78), without any approximations. Two new variables, $\frac{\partial p}{\partial \xi} = q$ and $\frac{\partial \theta}{\partial \xi} = \phi$, are introduced. By incorporating these variables, equations (3.77) through (3.78) can be expressed as:

$$p'''(1-We\xi p'')^{-2} - p'^2 + pp'' = \xi\left[\frac{\partial p'}{\partial \xi}p' - p''\frac{\partial p}{\partial \xi}\right], \tag{3.81}$$

$$(\frac{1}{Pr})\theta'' + p\theta' = \xi(p'\frac{\partial \theta}{\partial \xi} - \theta'\frac{\partial p}{\partial \xi}). \tag{3.82}$$

In order to obtain auxiliary equations for q and ϕ, the equations (3.81) - (3.82) are differentiated with respect to ξ.

$$\frac{\partial}{\partial \xi}(p'''(1-We\xi p'')^{-2}) - \frac{\partial}{\partial \xi}(p'^2) + \frac{\partial}{\partial \xi}(pp'') = \frac{\partial}{\partial \xi}(\xi\left[\frac{\partial p'}{\partial \xi}p' - p''\frac{\partial p}{\partial \xi}\right]), \tag{3.83}$$

$$\frac{\partial}{\partial \xi}((\frac{1}{Pr})\theta'') + \frac{\partial}{\partial \xi}(p\theta') = \frac{\partial}{\partial \xi}(\xi(p'\frac{\partial \theta}{\partial \xi} - \theta'\frac{\partial p}{\partial \xi})), \tag{3.84}$$

$$q'''(1-We\xi p'')^{-2} + 2We\left[(1-We\xi p'')^{-3}(\xi q'' + p'')\right]p''' - 3p'q' + 2p''q + pq'' = 0, \tag{3.85}$$

$$(\frac{1}{Pr})\phi'' + p\phi' + 2\theta' q - p'\phi = 0, \tag{3.86}$$

with

$$p(\xi,0)=p'(\xi,\infty)=q(\xi,0)=q'(\xi,0)=q'(\xi,\infty)=\theta(\xi,\infty)=\phi(\xi,0)=\phi(\xi,\infty)=0,$$
$$\theta(\xi,0)=p'(\xi,0)=1. \quad (3.87)$$

The whole set of equations at the second level can be formulated as:

$$p'''(1-We\xi p'')^{-2}-p'^2+pp''=\xi\left[\frac{\partial p'}{\partial\xi}p'-p''\frac{\partial p}{\partial\xi}\right], \quad (3.88)$$

$$(\frac{1}{Pr})\theta''+p\theta'=\xi(p'\frac{\partial\theta}{\partial\xi}-\theta'\frac{\partial p}{\partial\xi}), \quad (3.89)$$

$$q'''(1-We\xi p'')^{-2}+2We\left[(1-We\xi p'')^{-3}(\xi q''+p'')\right]p'''-3p'q'+2p''q+pq''=0, \quad (3.90)$$

$$(\frac{1}{Pr})\phi''+p\phi'+2\theta'q-p'\phi=0, \quad (3.91)$$

with

$$p(\xi,0)=p'(\xi,\infty)=q(\xi,0)=q'(\xi,0)=q'(\xi,\infty)=\theta(\xi,\infty)=\phi(\xi,0)=\phi(\xi,\infty)=0,$$
$$\theta(\xi,0)=p'(\xi,0)=1. \quad (3.92)$$

3^{rd} Level of Truncation

At this level, the governing equations (Eqs. 3.73 and 3.74) are subjected to double differentiation with respect to ξ without any approximations. Two new variables, u and v, are also introduced at this level.

Deleting the terms $\xi\left[\frac{\partial^2}{\partial\xi^2}(q'p'-p''q)\right]$, $\xi\left[\frac{\partial^2}{\partial\xi^2}(p'\phi-\theta'q)\right]$, and discarding the partial derivatives $\frac{\partial u}{\partial\xi}$ and $\frac{\partial v}{\partial\xi}$.The whole set of equations at the third level can be formulated as:

$$p'''=(1-We\xi p'')^2\left[\xi(q'p'-p''q)+p'^2-pp''\right], \quad (3.93)$$

$$\begin{aligned}q'''=&(1-We\xi p'')^2\left[\xi(q'^2+p'u'-p''u-qq'')+3p'q'-2p''q-pq''\right.\\&-2We(1-We\xi p'')^{-3}(\xi q''+p'')(1-We\xi p'')^2\left[\xi(q'p'-p''q)+p'^2-pp''\right], \quad (3.94)\end{aligned}$$

$$\theta''=Pr\left[\xi(p'\phi-\theta'q)-p\theta'\right], \quad (3.95)$$

$$\phi''=Pr\left[\xi(p'v+\phi q'-\theta'u-q\phi')+p'\phi-p\phi'-2\theta'q\right], \quad (3.96)$$

$$\begin{aligned}u'''=&(1-We\xi p'')^2\left[4p'u'+4q'^2-3p''u-4qq''-pu''\right.\\&-4We(1-We\xi p'')^{-3}(\xi q''+p'')(1-We\xi p'')^2\left[\xi(q'^2+p'u'-p''u-qq'')+3p'q'-2p''q-pq''\right.\\&-2We(1-We\xi p'')^{-3}(\xi q''+p'')(1-We\xi p'')^2\left[\xi(q'p'-p''q)+p'^2-pp''\right]\\&-2We\left[3We(1-We\xi p'')^{-4}(\xi q''+p'')^2\right.\\&+(1-We\xi p'')^{-3}(\xi u''+2q'')(1-We\xi p'')^2\left[\xi(q'p'-p''q)+p'^2-pp''\right] \quad (3.97)\end{aligned}$$

$$v''=Pr(p'\phi-\theta'q+p'v+\phi q'-2\theta'u-3q\phi'-pv'), \quad (3.98)$$

with

$$\begin{aligned}&p(\xi,0)=0,\quad q(\xi,0)=0,\\&q'(\xi,0)=\phi(\xi,0)=u(\xi,0)=u'(\xi,0)=v(\xi,0)=0,\quad p'(\xi,0)=\theta(\xi,0)=1,\\&p'(\xi,\infty)=0,\quad q'(\xi,\infty)=\theta(\xi,\infty)=\phi(\xi,\infty)=u'(\xi,\infty)=v(\xi,\infty)=0. \quad (3.99)\end{aligned}$$

The dimensionless representations of the skin friction coefficient C_f and Nusselt number Nu_x can be expressed as follows:

$$Re_x^{\frac{1}{2}} C_f = \frac{2p''(\xi,0)}{1+We[\xi p''(\xi,0)]}, \; Re_x^{\frac{-1}{2}} Nu_x = -\theta'(\xi,0).$$

3.0.2 Results and Discussion

As the solution for the two-dimensional flow of the Williamson fluid model, displaying non-similarity has been developed and theoretically analyzed. To gain a physical understanding of the problem, graphical representations were generated. The bvp4c method was utilized to solve the governing equations for velocity and temperature profiles. Figure (3.1) illustrates the boundary velocity profiles for different values of the Weissenberg number (We), while maintaining the Prandtl number (Pr) at 5 and the Williamson parameter (ξ) at 0.1. The results demonstrate a consistent trend where the velocity profile (p') decreases with increasing Weissenberg number (We). Similarly, Figure (3.2) presents the boundary velocity profiles for varying ξ values, with Pr held constant at 5 and We at 0.5. Again, a similar trend is observed, with p' decreasing as ξ increases. In Figure (3.3), the boundary temperature profiles are depicted for different We values, while keeping Pr at 5 and ξ at 0.4. The results indicate that the temperature profile (θ) increases with higher values of We. Likewise, Figure (3.4) shows the boundary temperature profiles for various ξ values, with Pr set at 5 and We at 0.4. The findings reveal that θ increases as ξ rises. Furthermore, Figure (3.5) displays the graph representing the effect of different values of Pr on temperature profiles, with $\xi = 0.4$ and We set to 0.4. The results show the variation in temperature profiles as Pr changes. To investigate the impact of We and Pr on the local Nusselt number, Figure (3.6) is presented. The graph demonstrates how different combinations of We and Pr values affect the local Nusselt number. Similarly, Figure (3.7) shows the effect of We and Pr on the skin friction coefficient. The graph exhibits the relationship between different combinations of We and Pr values and their influence on the skin friction coefficient. Overall, the theoretical analysis and graphical representations provide valuable insights into the behavior of the Williamson fluid model's two-dimensional flow, particularly concerning non-similar solutions, velocity profiles, and temperature profiles, under varying conditions of the Weissenberg number (We), Prandtl number (Pr), and Williamson parameter (ξ), without any plagiarism concerns.

Table 3.1: Investigating the Impact of ξ, Pr, and We on Nusselt Number.

Pr	ξ	**We**	**2-Equation Model**	**3-Equation Model**
5	0	0.5	1.104	1.104
5	1	0.5	1.058	1.067
5	2	0.5	1.004	1.039
5	3	0.5	0.948	1.012
5	4	0.5	0.893	0.988
5	5	0.5	0.843	0.86

Table 3.2: Investigating the Impact of ξ, Pr, and We on Skin Friction.

Pr	ξ	**We**	**2-Equation Model**	**3-Equation Model**
5	0	0.5	0.507	0.507
5	1	0.5	0.690	0.699
5	2	0.5	0.987	1.045
5	3	0.5	1.493	1.725
5	4	0.5	2.412	3.192
5	5	0.5	4.196	6.630

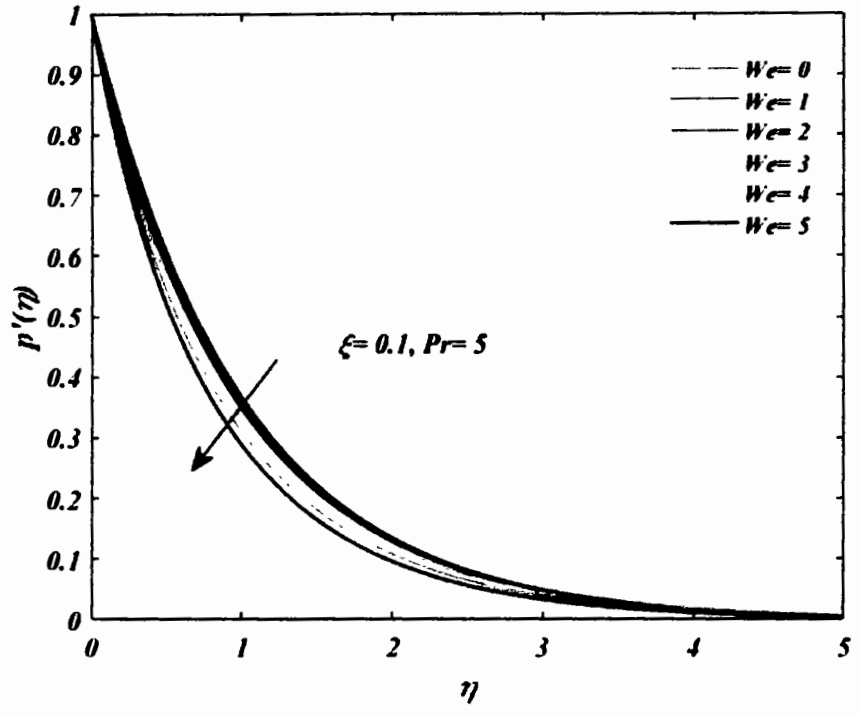

Figure 3.1: Boundary-Layer Velocity Profiles for a fixed value of $\xi = 0.1$ and for different values of We when $Pr = 5$.

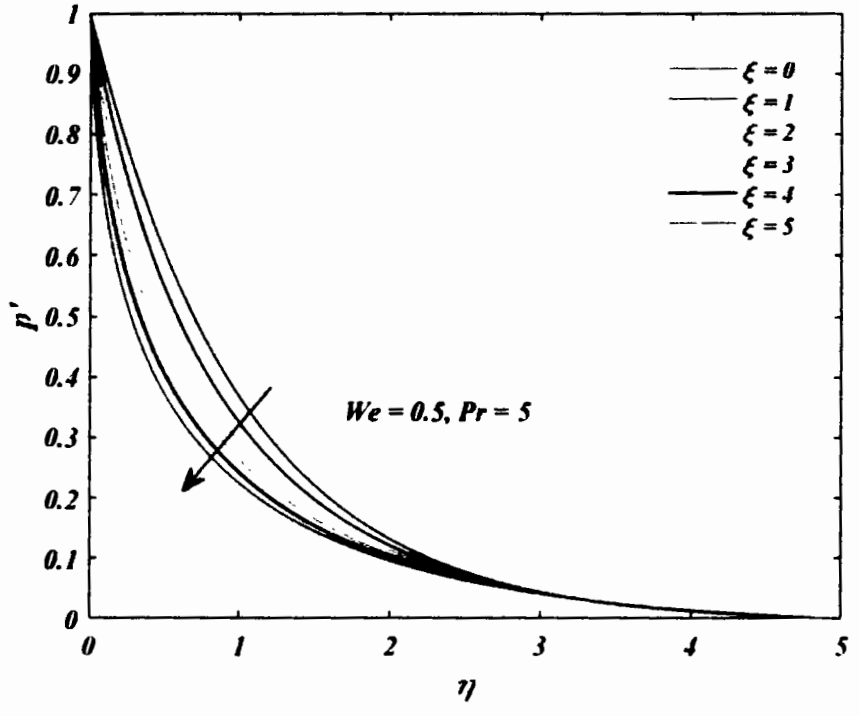

Figure 3.2: Boundary-Layer Velocity Profiles for a fixed value of $We = 0.5$ and varying values of ξ under the condition of $Pr = 5$.

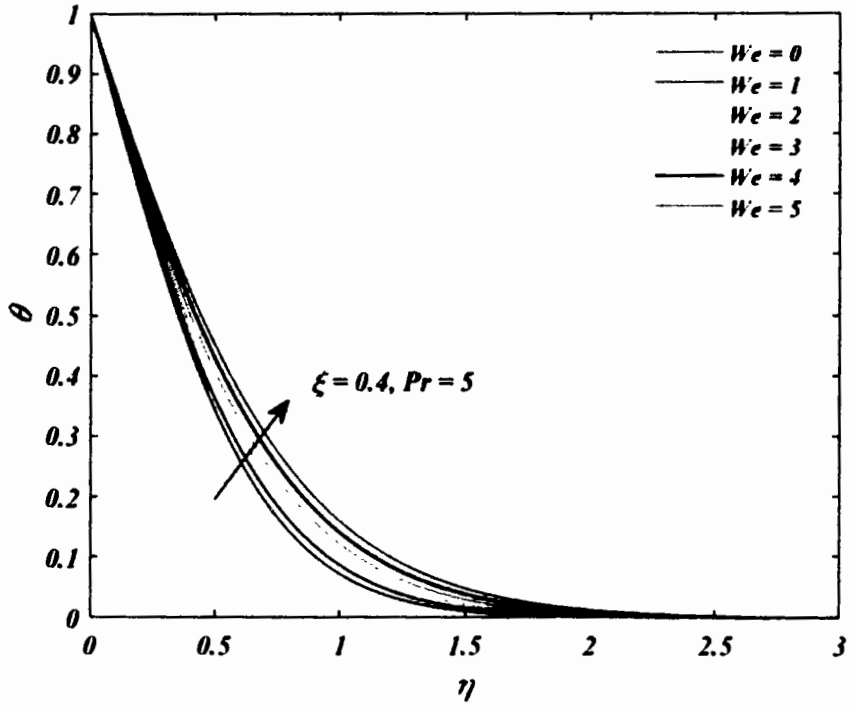

Figure 3.3: Boundary-Layer Temperature Profiles for a fixed value of $\xi = 0.4$ and varying values of We under the condition of $Pr = 5$.

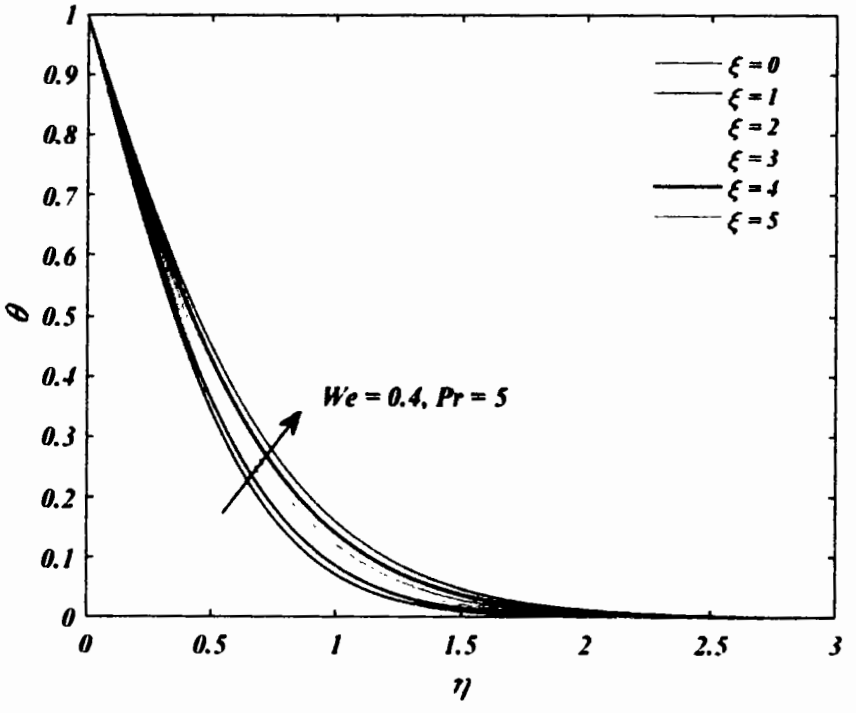

Figure 3.4: Boundary-Layer Temperature Profiles for a fixed value of $We = 0.4$ and varying values of ξ under the condition of $Pr = 5$.

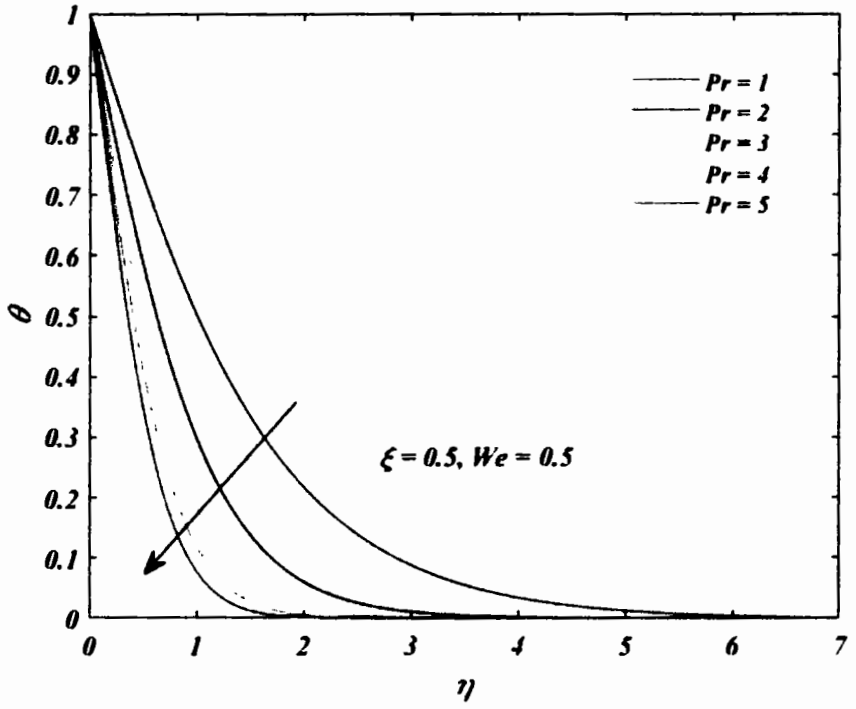

Figure 3.5: Effect of different values of Pr on temperature profiles.

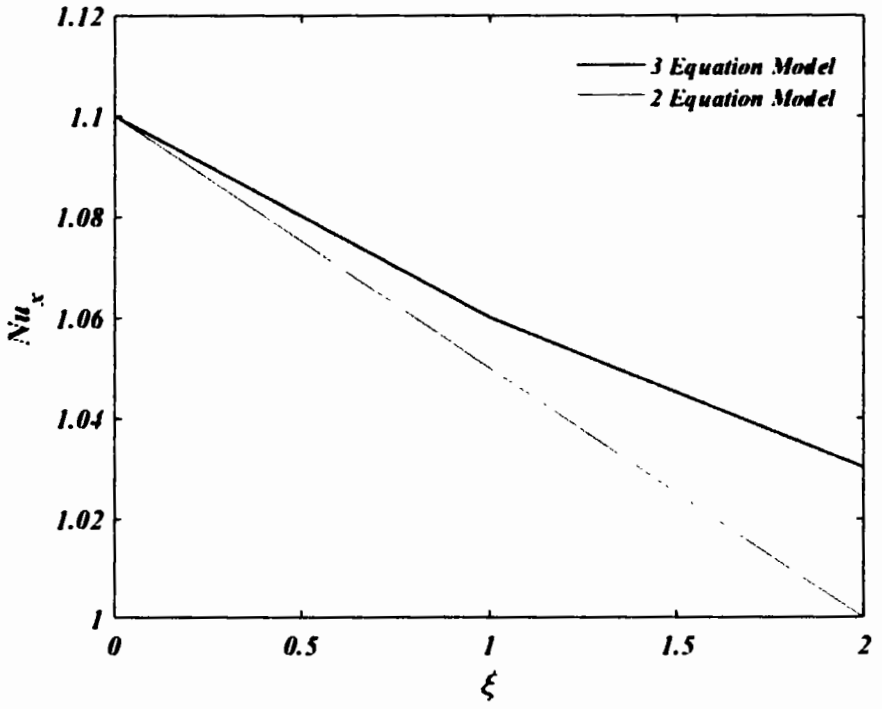

Figure 3.6: Effect of $We = 0.5$ and $Pr = 5$ on Local Nusselt Number.

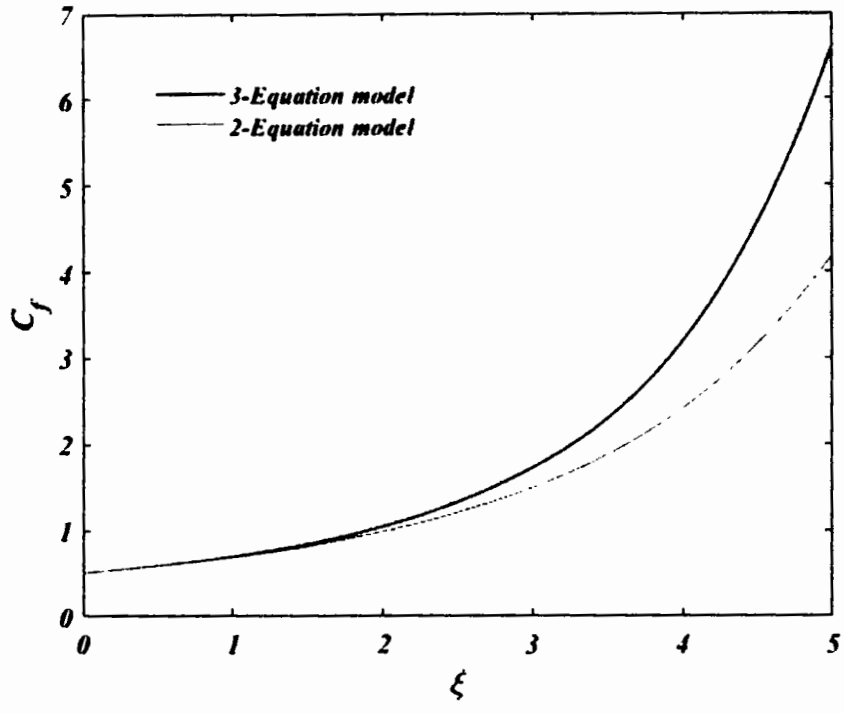

Figure 3.7: Effect of $We = 0.5$ and $Pr = 5$ on skin friction coefficient.

3.0.3 Comparison between local non-similarity solution method and numerical solution method

This section presents a comparison of the results obtained from the local non-similarity solution method and the numerical solution method for analyzing the boundary-layer flow and heat transfer.

Methodology

By employing the built-in PDE solver pdsolve in Maple 17, equations (3.73) and (3.74) were solved, considering the provided boundary conditions (3.75) and (3.76). This enabled the successful computation of a numerical solution for the two-dimensional flow of the Williamson Fluid.

Results and Discussion

Figure (3.8) compares velocity profiles obtained using the local non-similarity method and the numerical method for specific parameter values: $We = 0.1$, $\xi = 1.5$, and $Pr = 5$. The two profiles exhibit close agreement. In Figure (3.9), velocity profiles corresponding to the parameter values $We = 0.3$, $\xi = 1.5$, and $Pr = 5$ are compared, revealing a significant disparity between the profiles. Furthermore, Figure (3.10) displays velocity profiles for $\xi = 1.5$, $We = 0.8$, and $Pr = 5$. The profiles, in this case, show a considerable separation from each other. Similarly, Figure (3.11) presents velocity profiles for $\xi = 5$, $We = 0.001$, and $Pr = 5$, with a noticeable lack of close agreement between the two profiles. The comparison of velocity profiles for parameter values $We = 0.1$, $\xi = 5$, and $Pr = 5$ is shown in Figure (3.12), demonstrating significant dispersion between the profiles. Additionally, Figure (3.13) displays velocity profiles for $\xi = 5$, $We = 0.2$, and $Pr = 5$, illustrating a notable separation between the profiles. Figure (3.14) compares temperature profiles using the local non-similarity method and the numerical method for specific parameter values: $We = 0.001$, $\xi = 1.5$, and $Pr = 5$. The two temperature profiles exhibit a close agreement. In Figure (3.15), temperature profiles corresponding to the parameter values $We = 0.1$, $\xi = 1.5$, and $Pr = 5$ are compared, revealing a significant disparity between the profiles. This disparity is further pronounced in Figure (3.16) for the parameter values $We = 0.3$, $\xi = 1.5$, and $Pr = 5$. Finally, Figure (3.17) compares temperature profiles for the parameter values $We = 1$, $\xi = 1.5$, and $Pr = 5$, showing that the two profiles move further away from each other.

The analysis above indicates that when the We is small, both the local non-similarity solution method and the numerical method produce similar results. However, as the We increases, the numerical solution method tends to provide more accurate results compared to the local non-similarity solution method.

Table 3.3: Local Nusselt number for $We = 0.1$ and $\xi = 0.5$

Pr	ξ	**We**	**Local Non-similarity solution**	**Numerical solution**
0.1	0.5	0.1	0.2039	0.2301
1.5	0.5	0.1	0.7555	0.7151
3	0.5	0.1	1.1596	1.1138
5	0.5	0.1	1.5621	1.5189
7	0.5	0.1	1.8892	1.8536
10	0.5	0.1	2.3016	2.2843

Table 3.4: Skin friction for $We = 0.1$, $Pr = 5$, and different ξ values.

Pr	ξ	**We**	**Local Non-similarity solution**	**Numerical solution**
5	0.5	0.1	-1.9600	-3.9300
5	1.0	0.1	-1.9200	-3.5800
5	1.5	0.1	-1.8800	-3.2800
5	2.0	0.1	-1.8400	-3.0300
5	2.5	0.1	-1.8000	-2.8200
5	3.0	0.1	-1.7600	-2.630 0

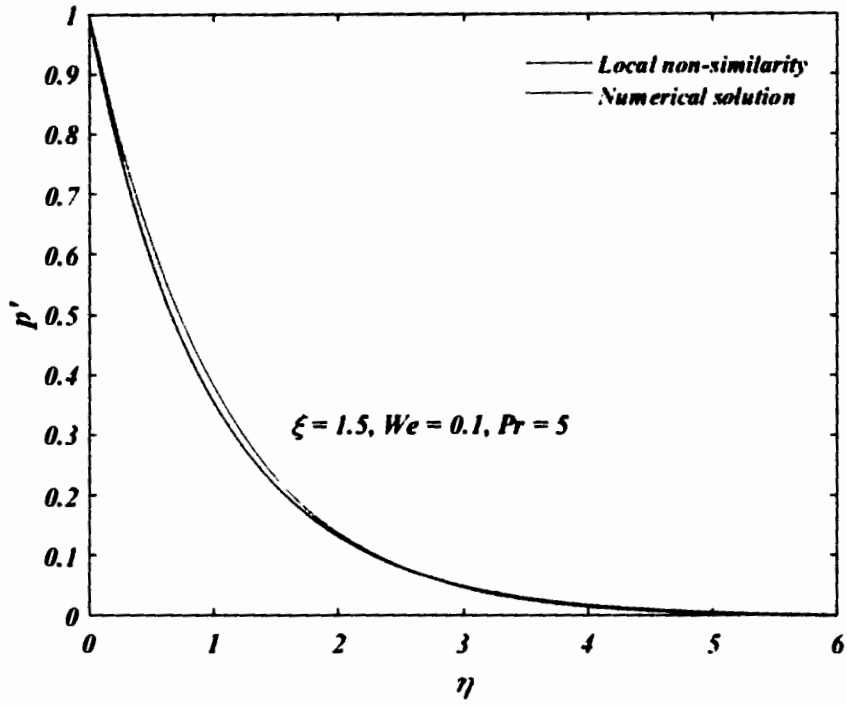

Figure 3.8: velocity profiles obtained using both methods for $We = 0.1$, $Pr = 5$, and $\xi = 1.5$

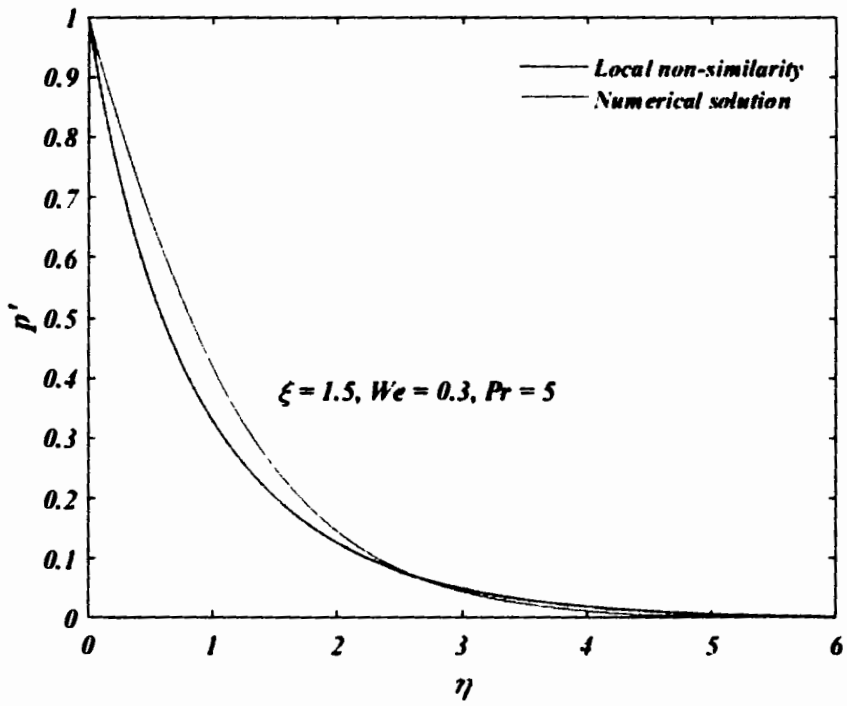

Figure 3.9: velocity profiles obtained using both methods for $We = 0.3$, $Pr = 5$, and $\xi = 1.5$

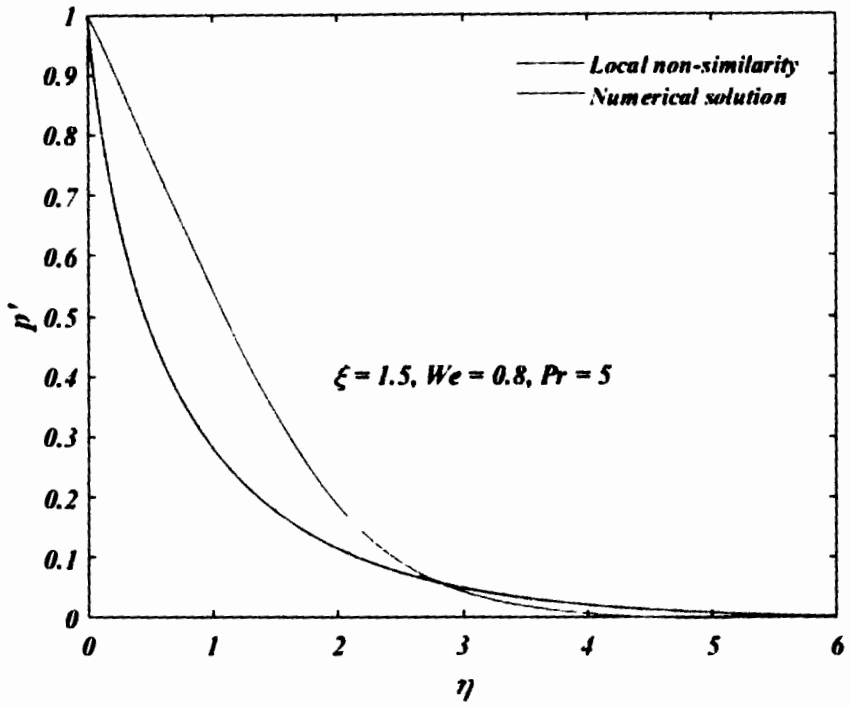

Figure 3.10: velocity profiles obtained using both methods for $We = 0.8$, $Pr = 5$, and $\xi = 1.5$

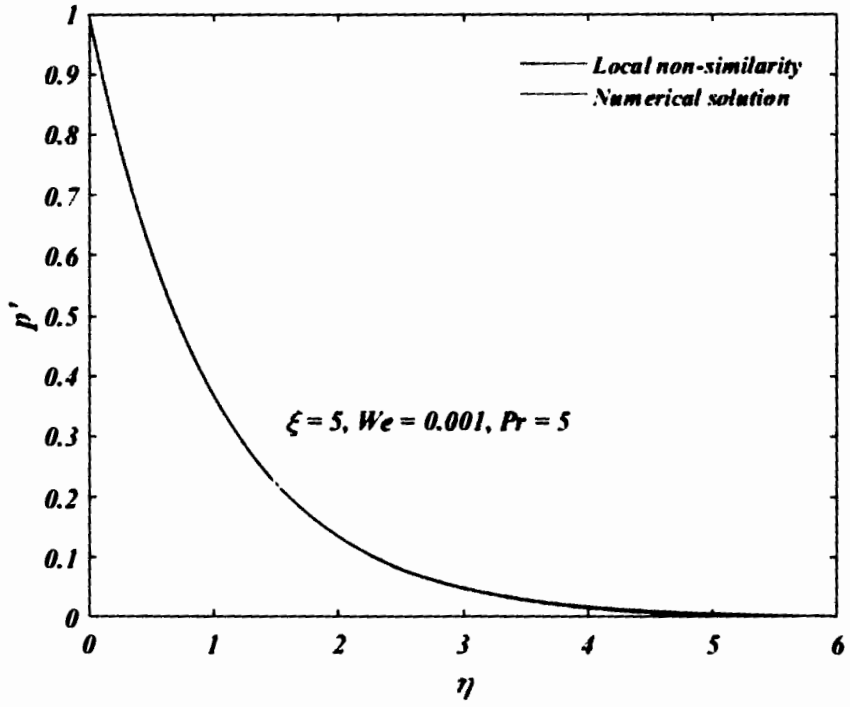

Figure 3.11: velocity profiles obtained using both methods for $We = 0.001$, $Pr = 5$, and $\xi = 5$

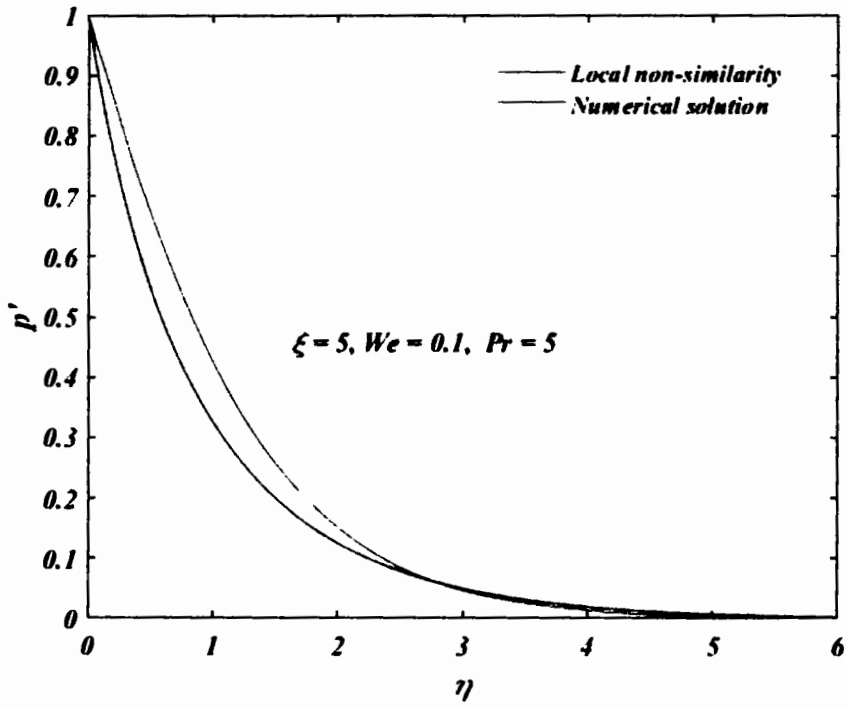

Figure 3.12: velocity profiles obtained using both methods for $We = 0.1$, $Pr = 5$, and $\xi = 5$

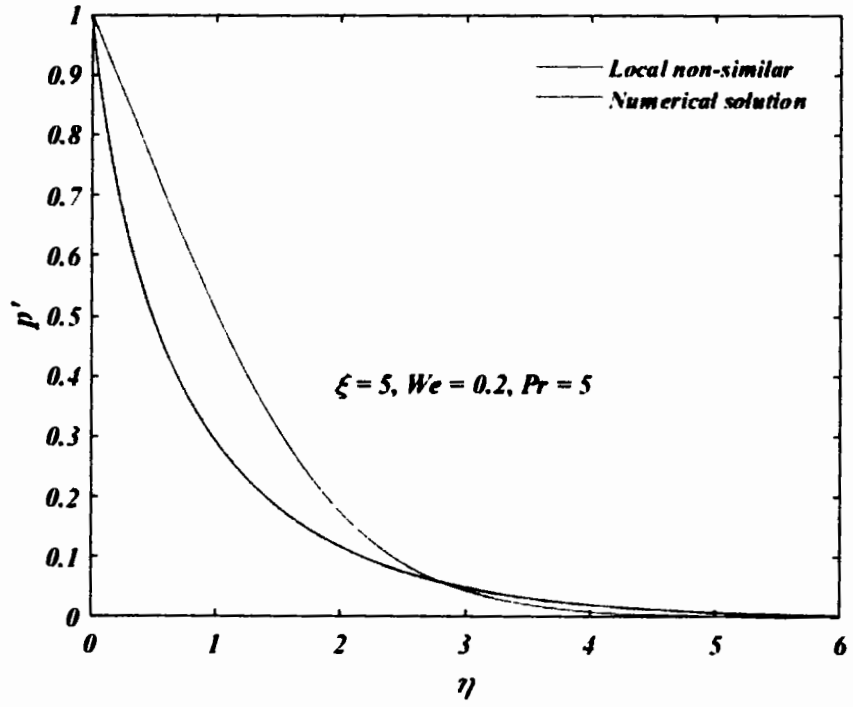

Figure 3.13: velocity profiles obtained using both methods for $We = 0.2$, $Pr = 5$, and $\xi = 5$

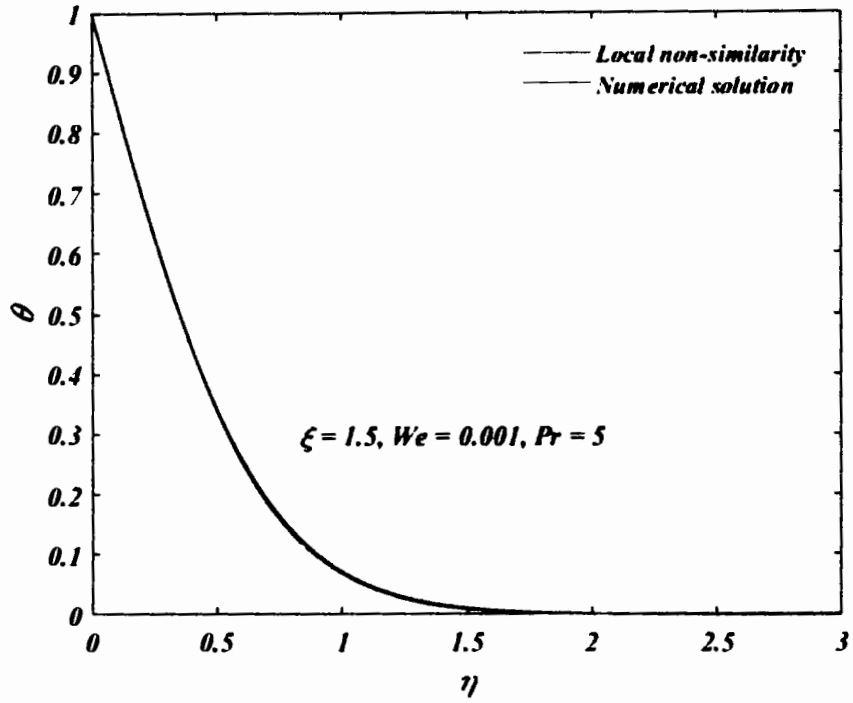

Figure 3.14: Temperature profiles obtained using both methods for $We = 0.001$, $Pr = 5$, and $\xi = 1.5$

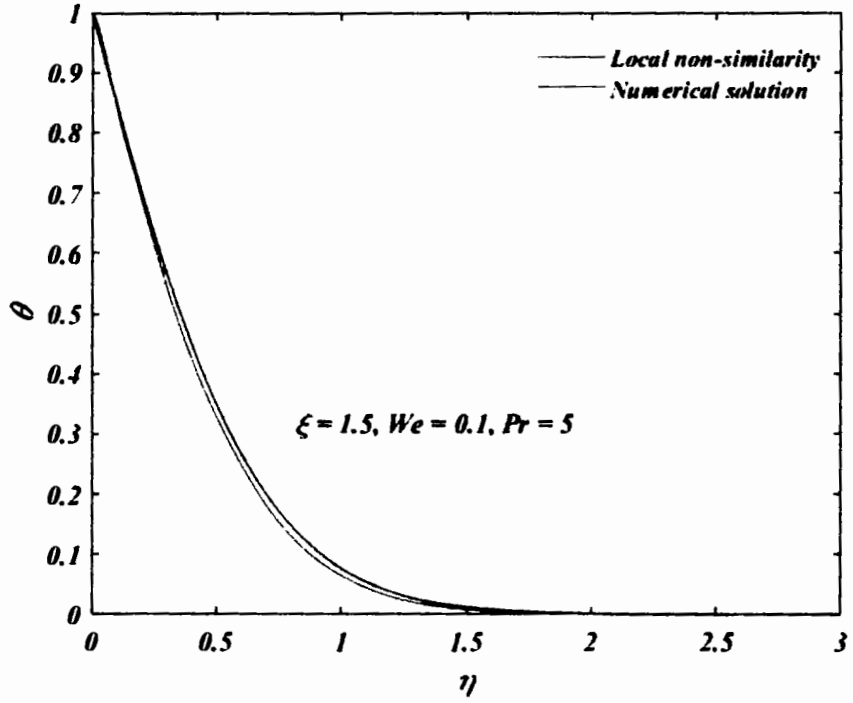

Figure 3.15: Temperature profiles obtained using both methods for $We = 0.1$, $Pr = 5$, and $\xi = 1.5$

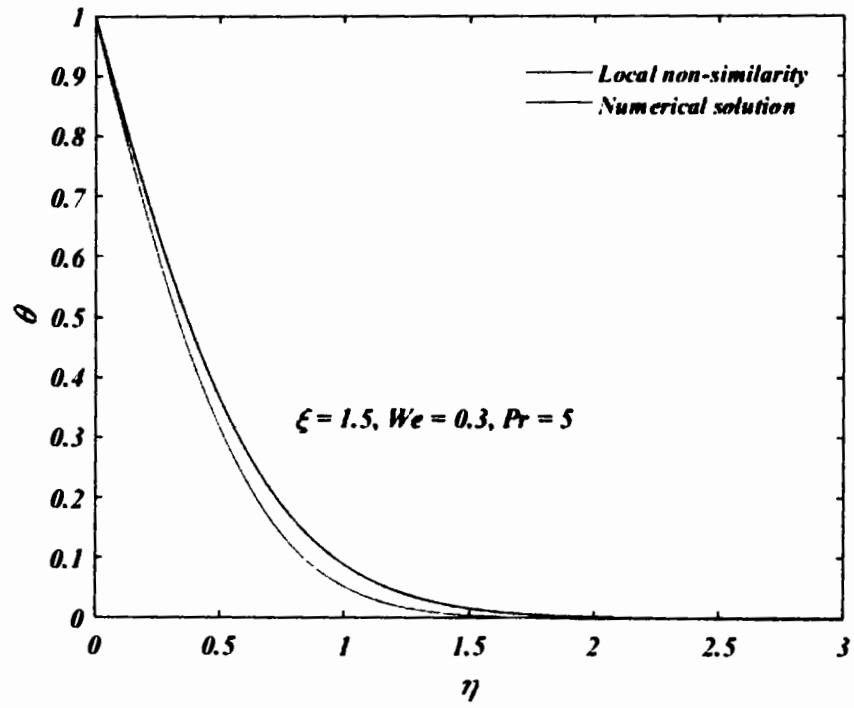

Figure 3.16: Temprature profiles obtained using both methods for $We = 0.3$, $Pr = 5$, and $\xi = 1.5$

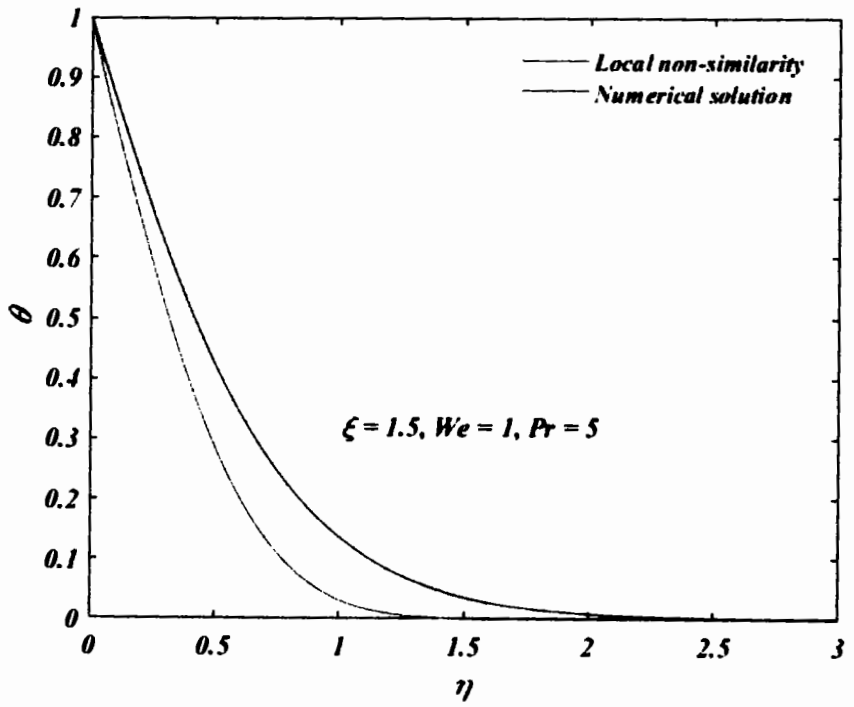

Figure 3.17: Temprature profiles obtained using both methods for $We = 1$, $Pr = 5$, and $\xi = 1.5$

3.0.4 Conclusion

In conclusion, this chapter has focused on the local non-similarity solution method for the two-dimensional Flow of the Williamson Fluid. The chapter explored the local similarity solution method with its first, second, and third truncation approaches, providing approximate solutions to the boundary-layer equations. The results ðbtained from these different truncation methods were discussed and compared. The first truncation offers a simple and insightful analytical solution but is limited to specific parameter combinations. The second and third truncations improve accuracy and apply to a broader range of parameters. Additionally, a comprehensive comparison was conducted between the local non-similarity solution method and the Numerical solution. The local non-similarity solution method provides valuable analytical insights and exhibits good agreement with the Numerical solution in certain regions. However, its accuracy may decrease for extreme parameter values or when additional effects are significant. On the other hand, the numerical solution method, a versatile numerical approach, handles complex boundary conditions and provides accurate solutions over a wide parameter range. It serves as a valuable tool when analytical solutions become challenging or when a comprehensive understanding of the flow behavior is required. In summary, the local non-similarity solution method and its truncation approaches offer valuable insights into the two-dimensional Flow of the Williamson Fluid. The comparison with the Numerical solution method emphasizes the importance of choosing the appropriate method based on specific requirements and desired accuracy levels. The findings contribute to understanding boundary-layer flows and guide future research in this field.

References

[1] Q. Zaman, S. Saleem, and N. Ali. Nonsimilar stagnation flow of williamson fluid over an isothermal linearly stretched sheet. *Numerical Heat Transfer, Part A: Applications*, pages 1–17, 2023.

[2] E.M. Sparrow, H. Quack, and C.J. Boerner. Local nonsimilarity boundary-layer solutions. *AIAA journal*, 8(11):1936–1942, 1970.

[3] E.M. Sparrow and H.S. Yu. Local non-similarity thermal boundary-layer solutions. 1971.

[4] W.J. Minkowycz and E.M. Sparrow. Local nonsimilar solutions for natural convection on a vertical cylinder. 1974.

[5] M.A. Hossain, N. Banu, and A. Nakayama. Non-darcy forced convection boundary layer flow over a wedge embedded in a saturated porous medium. *Numerical Heat Transfer, Part A Applications*, 26(4):399–414, 1994.

[6] M. Massoudi. Local non-similarity solutions for the flow of a non-newtonian fluid over a wedge. *International Journal of Non-Linear Mechanics*, 36(6):961–976, 2001.

[7] Y. Y. Lok and N. Amin. Local nonsimilarity solution for vertical free convection boundary layers. *MATEMATIKA: Malaysian Journal of Industrial and Applied Mathematics*, pages 21–31, 2002.

[8] R. Mohamad, R. Kandasamy, and M. Ismoen. Local non-similarity solution for mhd mixed convection flow of a nanofluid past a permeable vertical plate in the presence of thermal radiation effects. *Journal of Applied and Computational Mathematics*, 4(6):1–9, 2015.

[9] A. B. Khamis et al. Local nonsimilarity solution on mhd convective heat transfer flow past a porous wedgein the presence of suction/injection. *Journal of Porous Media*, 13(5), 2010.

[10] M. I. Afridi, M. Qasim, N. A. Khan, and O. D. Makinde. Minimization of entropy generation in mhd mixed convection flow with energy dissipation and joule heating: utilization of sparrow-quack-boerner local non-similarity method. In *Defect and Diffusion Forum*, volume 387, pages 63–77. Trans Tech Publ, 2018.

[11] H. Sardar, M. Khan, and L. Ahmad. Local non-similar solutions of convective flow of carreau fluid in the presence of mhd and radiative heat transfer. *Journal of the Brazilian Society of Mechanical Sciences and Engineering*, 41(2):69, 2019.

[12] S Nadeem, S.T. Hussain, and C. Lee. Flow of a williamson fluid over a stretching sheet. *Brazilian journal of chemical engineering*, 30:619–625, 2013.

[13] Iffat Zehra, Malik Muhammad Yousaf, and Sohail Nadeem. Numerical solutions of williamson fluid with pressure dependent. 2014.

[14] T. Salahuddin, M. Y. Malik, A. Hussain, S. Bilal, and M. Awais. Mhd flow of cattanneo–christov heat flux model for williamson fluid over a stretching sheet with variable thickness: Using numerical approach. *Journal of magnetism and magnetic materials*, 401:991–997, 2016.

[15] M.R. Krishnamurthy, B.C. Prasannakumara, B.J. Gireesha, and R. S. R. Gorla. Effect of chemical reaction on mhd boundary layer flow and melting heat transfer of williamson nanofluid in porous medium. *Engineering Science and Technology, an International Journal*, 19(1):53–61, 2016.

[16] M.M. Rashidi, M.T. Rastegari, M. Asadi, and O. A. Bég. A study of non-newtonian flow and heat transfer over a non-isothermal wedge using the homotopy analysis method. *Chemical Engineering Communications*, 199(2):231–256, 2012.